Topological Effects on Separation of Alkane Isomers in Metal-Organic Frameworks

SAND2020-7684C

N. Scott Bobbitt, Andrew S. Rosen, and Randall Q. Snurr

Northwestern University
Sandia National Laboratories

2020 ACS Virtual Fall Meeting
August 2020

SAND2019-13769 C

Sandia National Laboratories is a multi-mission laboratory managed and operated by National Technology and Engineering Solutions of Sandia, LLC., a wholly owned subsidiary of Honeywell International, Inc., for the U.S. Department of Energy's National Nuclear Security Administration under contract DE-NA0003525.

Bobbitt, Rosen, Snurr, Fluid Phase Equilibria, 519, 112642, 2020

How did I get here?

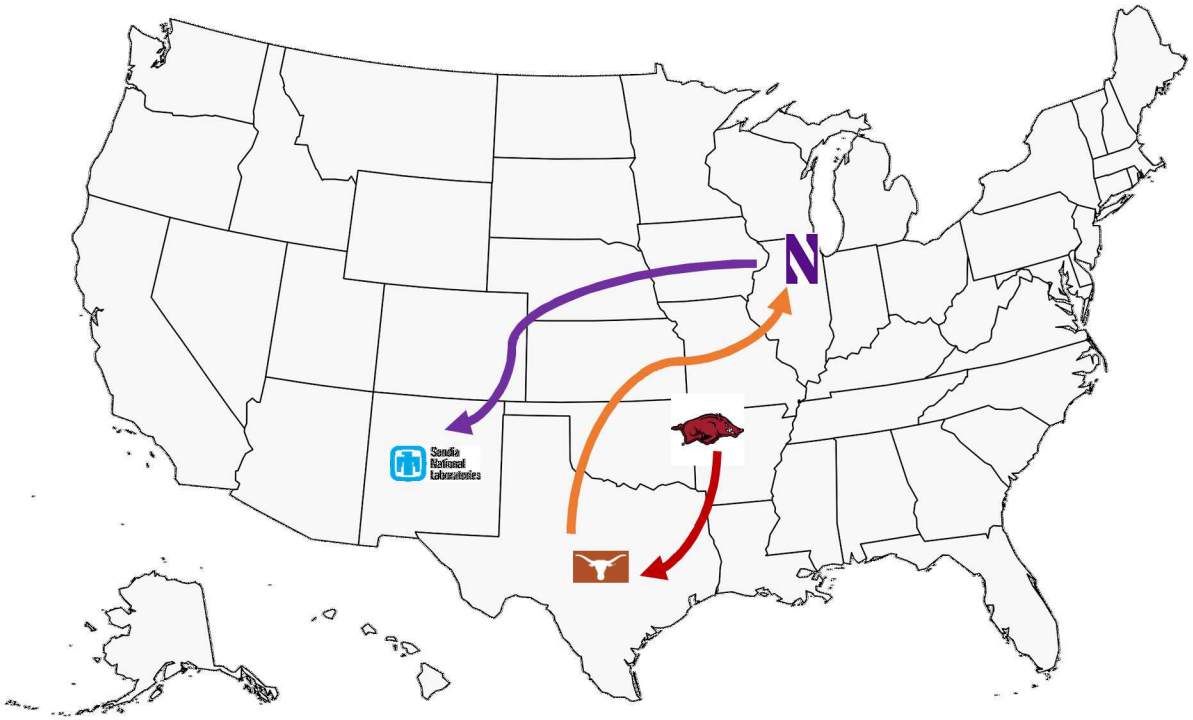

2008-2010: Undergraduate research with Dr. King at University of Arkansas

Gas chromatography measurements of properties of biodiesel

2010-2015: PhD student at University of Texas at Austin

DFT calculations for electronic structure of nanoparticles

2015-2019: postdoc at Northwestern University

molecular simulation for gas storage and separations in porous materials

2019-present: postdoc at Sandia National Labs, New Mexico

molecular dynamics simulations for materials discovery

Where it all began

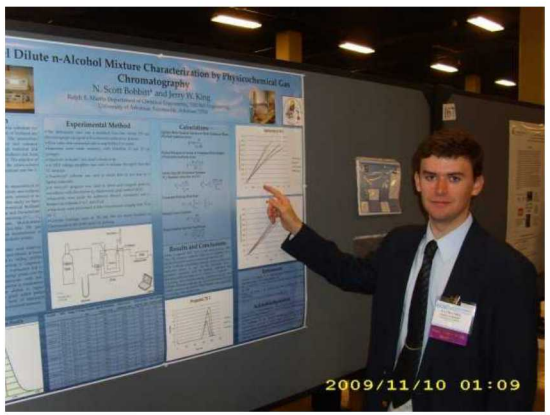

AIChE 2009

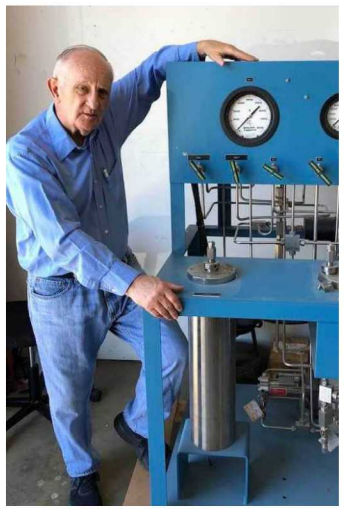

Congratulations to Jerry King!
2020 Spencer Award winner

Alkane Isomers

n-butane isobutane

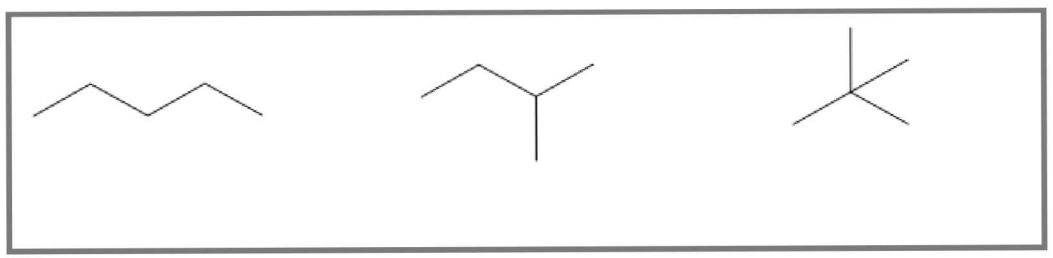

n-pentane 2-methylbutane 2,2-dimetylpropane (neopentane)

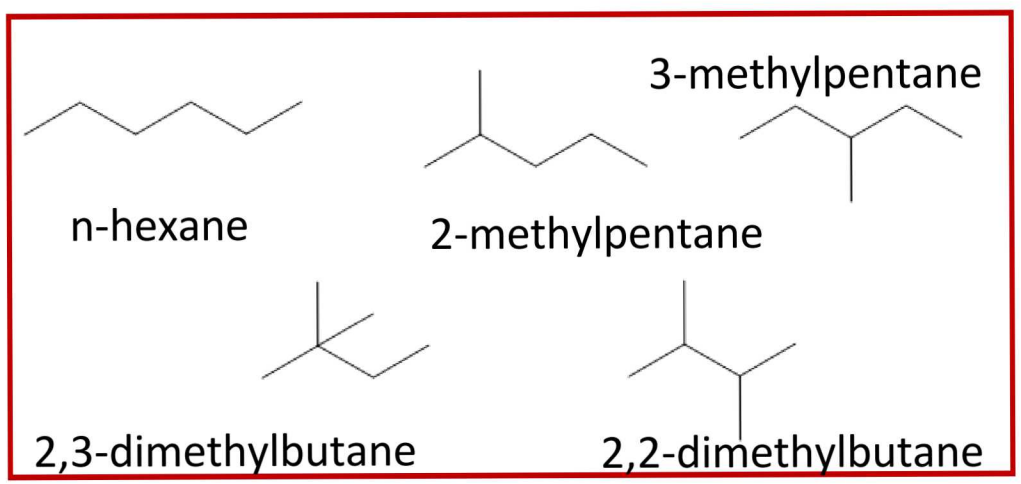

Isomer	Research Octane #
n-hexane	25
2-methylpentane	73
3-methylpentane	75
22-dimethylbutane	92
23-dimethylbutane	104

J. Combustion, ID 8406754, 2018

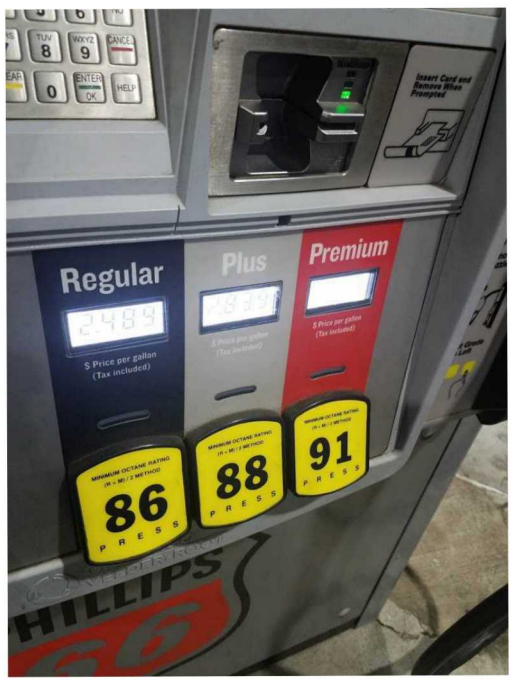

Branched isomers of hexane are key component of high-octane gasoline.

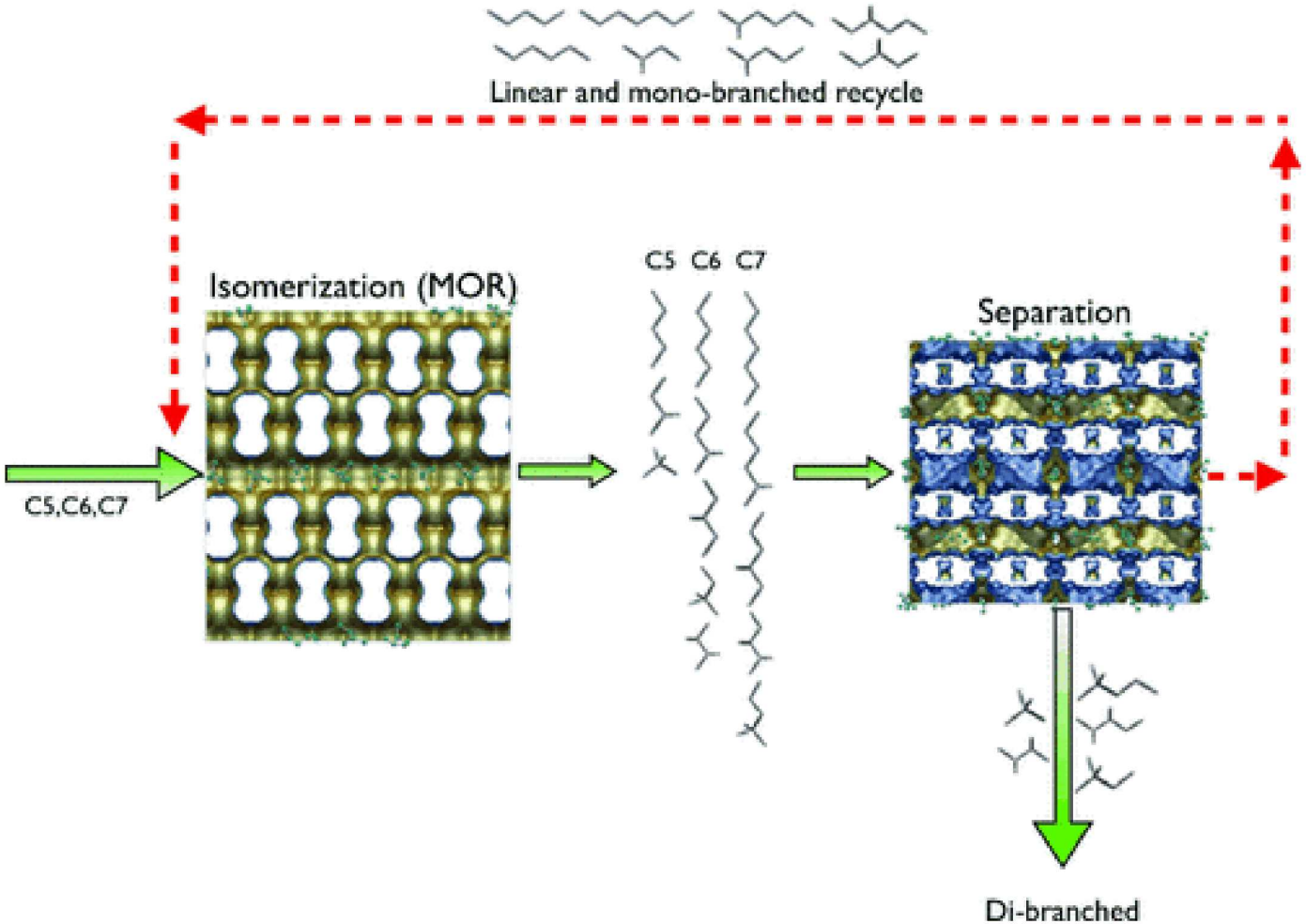

Dubbeldam, Angew. Chem. Int. Ed., 51, 11867-11871, 2012

Gasoline is enriched by separating linear and branched alkanes and feeding back into an isomerization process.

It is advantageous to find a solid sorbent (eg MOF, zeolites) that can achieve this separation with a high degree of selectivity and capacity.

Isomer	B.P (˚C)
n-hexane	68.7
2-methylpentane	63.3
3-methylpentane	60.3
22-dimethylbutane	58.0
23-dimethylbutane	49.7

Distillation is difficult and expensive.
10-15% of world energy consumption.

MOFs offer diverse pore shapes and sizes. We can choose a MOF to separate linear and branched isomers selectively based on shape.

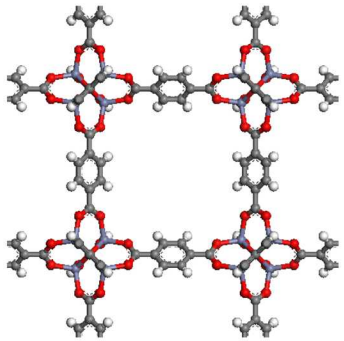

MOF-5

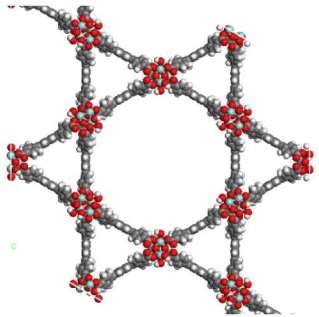

NU-1000

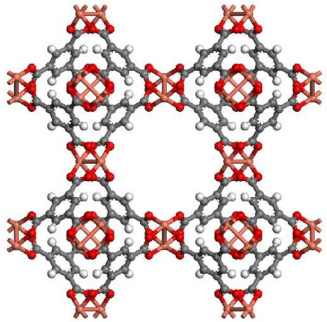

HKUST-1

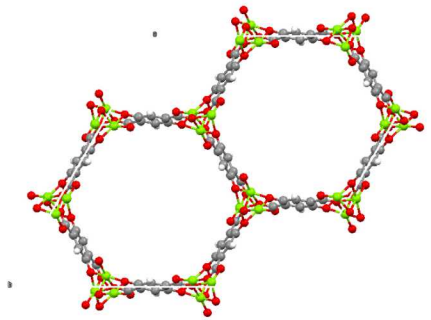

MOF-74

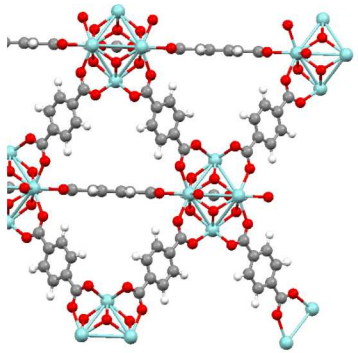

UiO-66

Shape-selective pores

Mason, future chemical engineer

Catalysis

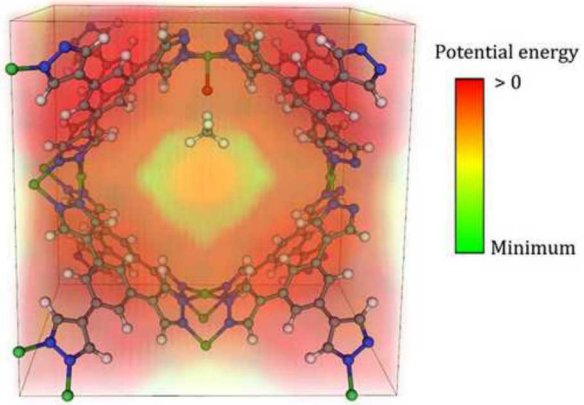

Rosen, J. Comp. Chem., 40, 1305-1318, 2019

Gas Storage

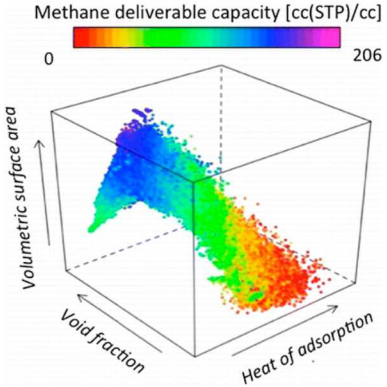

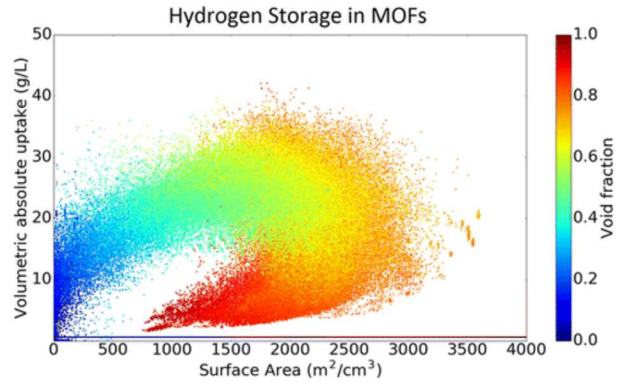

Gomez-Gualdron, J. Phys. Chem. C., 118, 6941-6951, 2014
Bobbitt, J. Phys. Chem. C, 120, 27328-27341, 2016

Nodes/Metals

Linkers

TUNABLE PROPERTIES

Functional Groups

Topology

Toxic Gas Capture

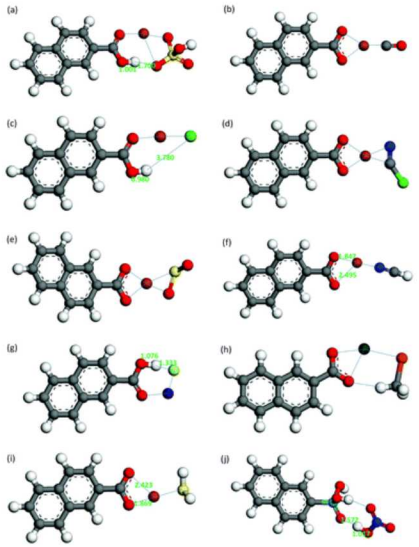

Kim, PCCP, 19, 31766-31772, 2017

Refrigeration

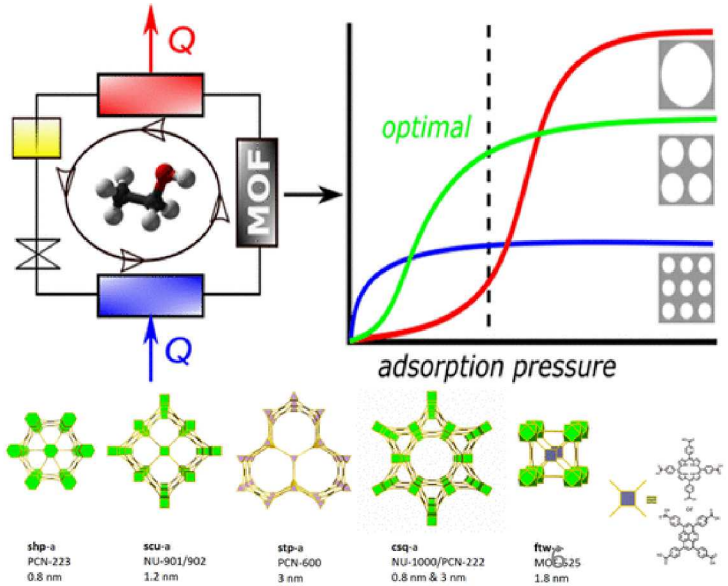

Chen, Chem. Mater., 31, 2702-2706, 2019

Many different combinations of nodes, linkers, and topologies can be used to form unique MOFs.

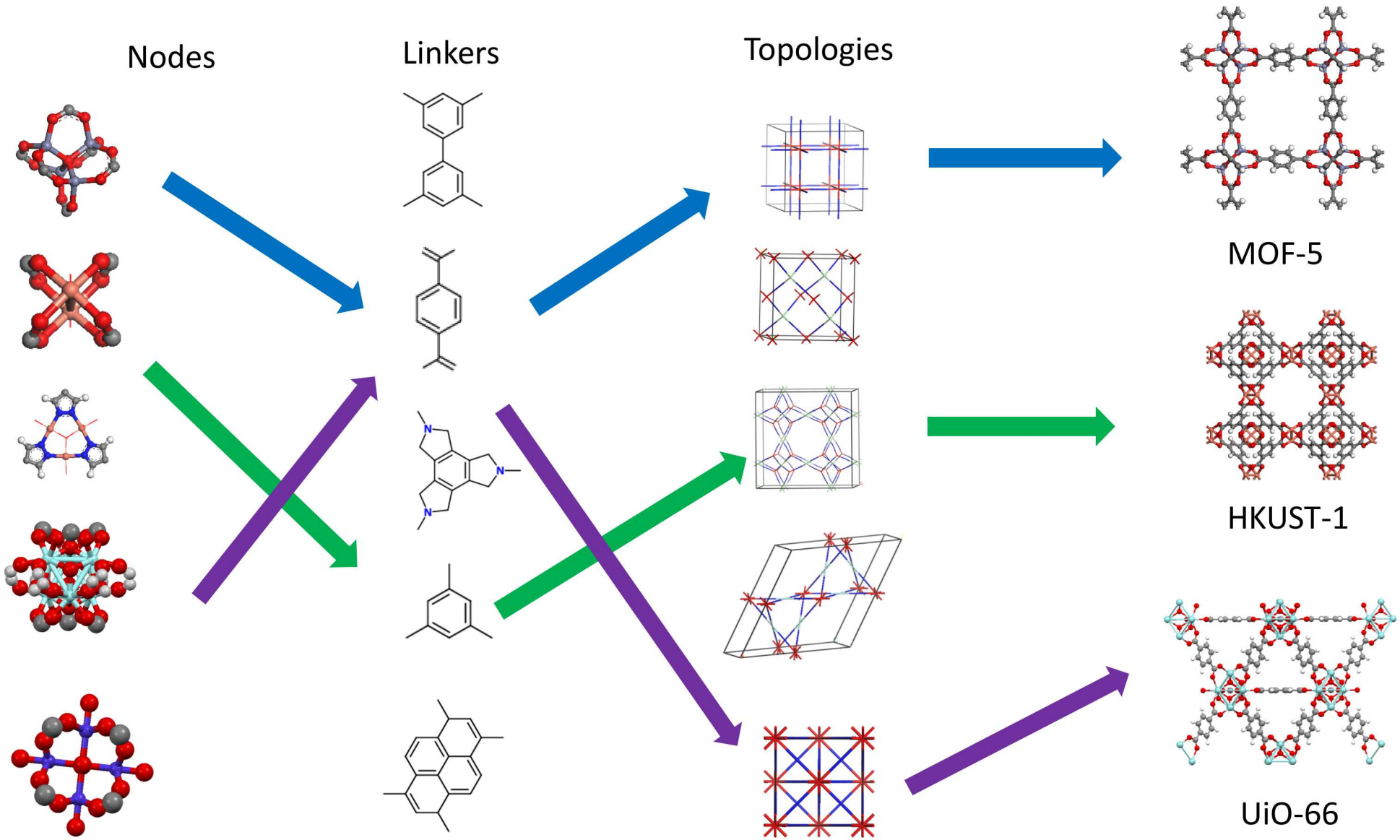

The same nodes and linkers can be combined in different topological networks to form unique MOFs with the same chemical formula.

Nodes

Linkers

Topologies

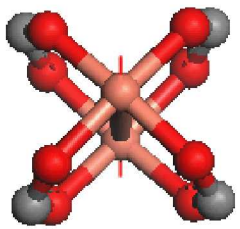

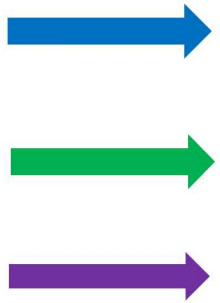

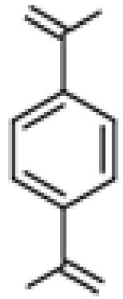

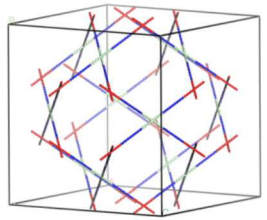

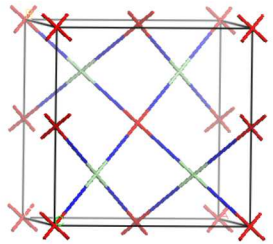

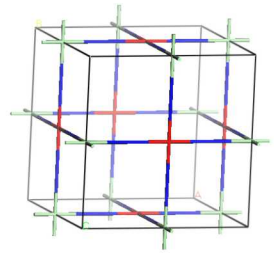

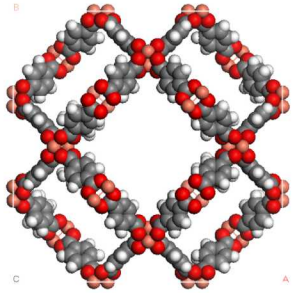

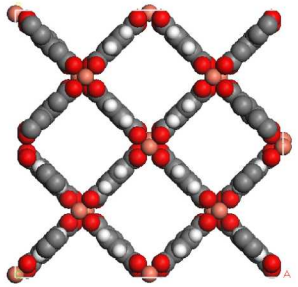

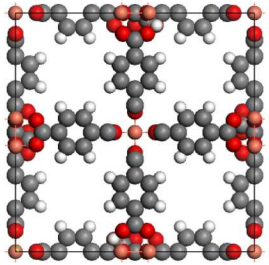

$CuC_8H_4O_4$

$CuC_8H_4O_4$

$CuC_8H_4O_4$

Polymorphs

Polymorphs are families of MOFs that contain the same nodes and linkers but arranged in different topologies.

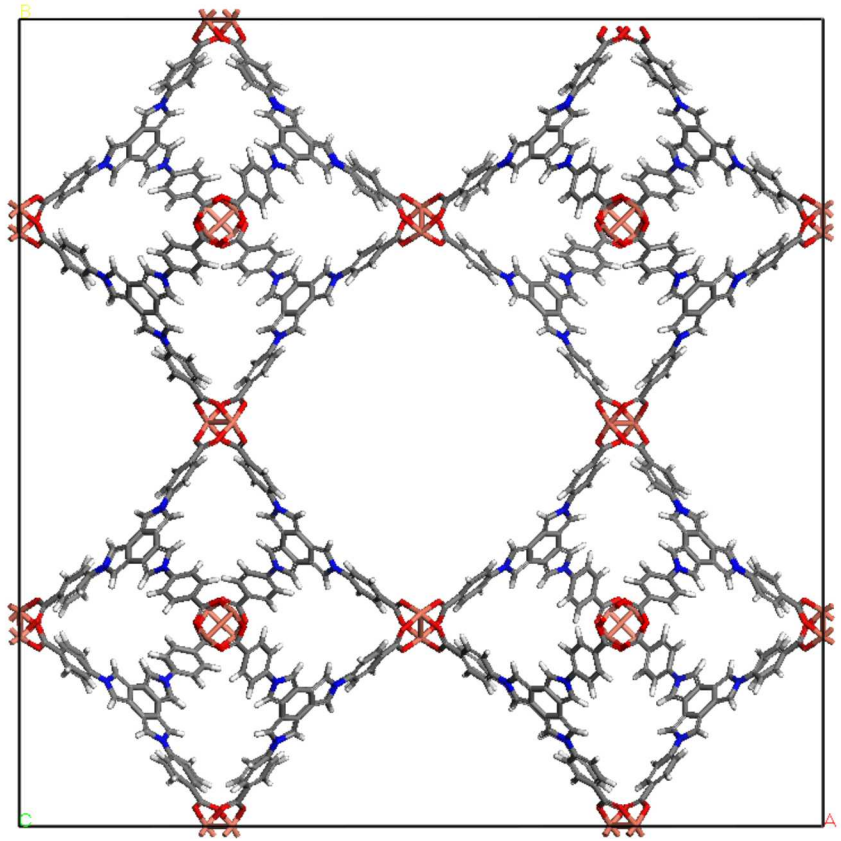

tbo

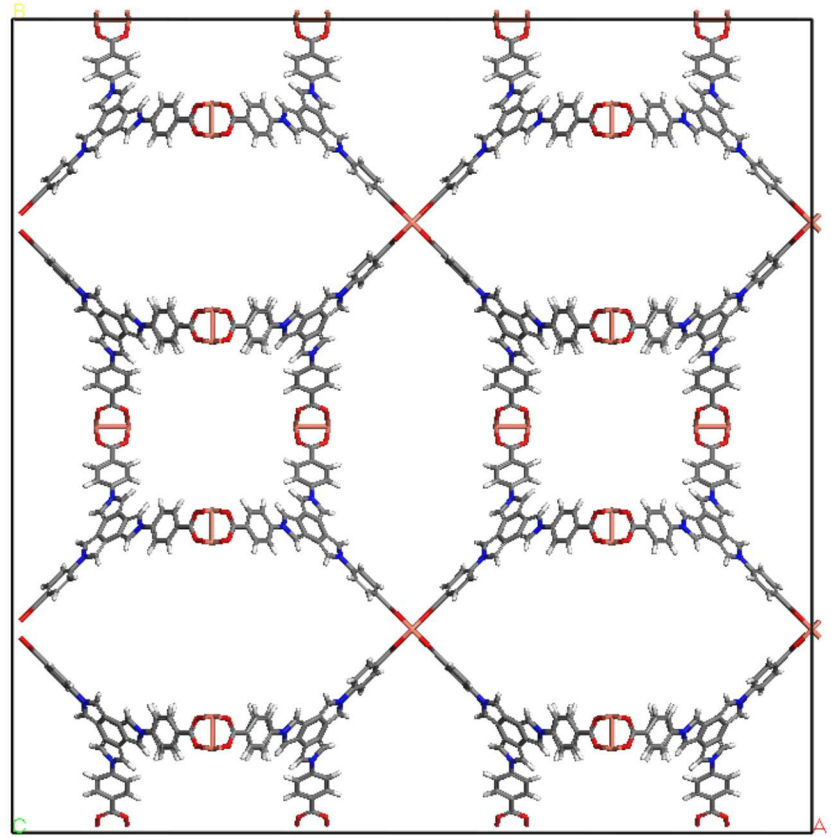

pto

I have selected four families of polymorphs that consist of 38 MOFs from the Tobacco database.

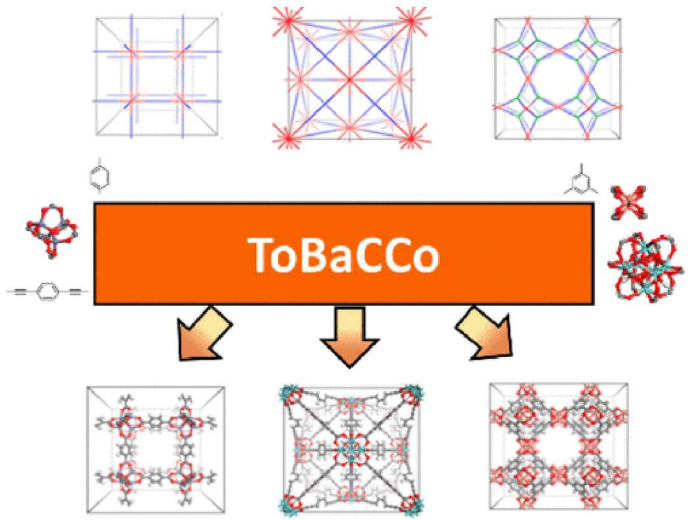

Colon, Gomez-Gualdron, Snurr, Cryst. Growth Des., 17, 5801-5810, 2017

Polymorph families:

dia/lcs/sod

lvt/nbo/rhr

tbo/pto

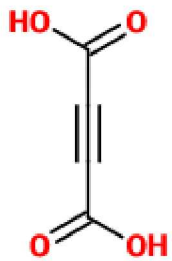

L3

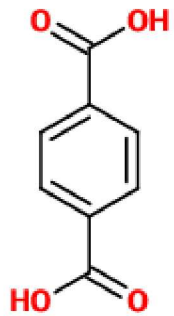

L12

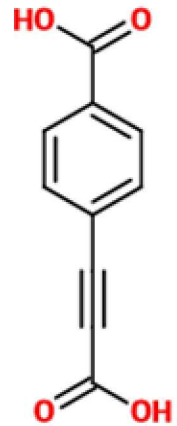

L20

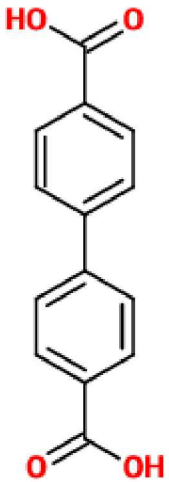

L24

ssa/ssb

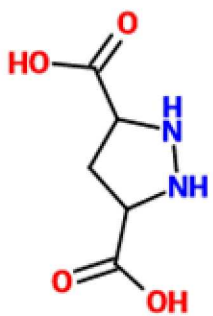

L4

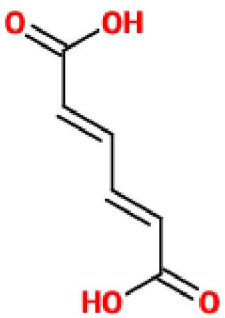

L15

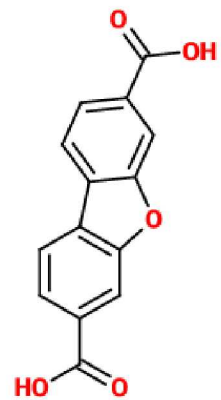

L21

Computational details

1. Monte Carlo simulations were performed in RASPA

2. We used the TraPPE model for alkanes and LJ parameters from UFF for MOFs.

3. MOF structures are kept rigid.

4. 20,000 cycles for Henry calculations and 100,000 total cycles (50k initialization-50k production) for GCMC using configurational biasing

For further details see Chung et al., Chem. Mater. 29, 6315-6328, 2017

Henry constants
mol/kg/Pa

nbo_L12 shows great affinity for n-hexane over branched isomers

MOF	C4	isobutane	C5	neopentane	2-methylbutane	C6	2-methylpentane	3-methylpentane	22-dimethylbutane	23-dimethylbutane
dia_L_12	7.6E-05	6.3E-05	1.8E-04	5.9E-05	1.3E-04	4.0E-04	3.1E-04	2.8E-04	1.8E-04	2.3E-04
dia_L_20	5.4E-05	4.5E-05	1.1E-04	4.2E-05	8.6E-05	2.3E-04	1.8E-04	1.7E-04	1.1E-04	1.4E-04
dia_L_24	7.0E-05	5.8E-05	1.5E-04	5.3E-05	1.2E-04	3.3E-04	2.6E-04	2.3E-04	1.5E-04	2.0E-04
dia_L_3	4.9E-05	4.2E-05	1.0E-04	4.0E-05	8.1E-05	2.1E-04	1.7E-04	1.6E-04	1.1E-04	1.4E-04
lcs_L_12	8.6E-05	7.1E-05	2.1E-04	6.6E-05	1.6E-04	5.1E-04	3.9E-04	3.6E-04	2.2E-04	3.0E-04
lcs_L_20	5.5E-05	4.6E-05	1.2E-04	4.3E-05	9.0E-05	2.4E-04	1.9E-04	1.7E-04	1.2E-04	1.5E-04
lcs_L_24	7.0E-05	5.8E-05	1.6E-04	5.4E-05	1.2E-04	3.5E-04	2.7E-04	2.5E-04	1.5E-04	2.1E-04
lcs_L_3	5.4E-05	4.6E-05	1.2E-04	4.5E-05	9.3E-05	2.5E-04	2.1E-04	1.9E-04	1.3E-04	1.6E-04
lvt_L_12	3.5E-03	3.4E-03	2.5E-02	9.1E-03	3.0E-02	1.6E-01	1.9E-01	2.4E-01	2.0E-01	3.1E-01
lvt_L_20	2.4E-04	2.1E-04	8.7E-04	2.5E-04	6.8E-04	3.1E-03	2.5E-03	2.3E-03	1.5E-03	1.9E-03
lvt_L_24	1.5E-04	1.4E-04	4.3E-04	1.6E-04	3.8E-04	1.2E-03	1.1E-03	1.0E-03	7.4E-04	9.3E-04
lvt_L_3	6.3E-04	6.3E-04	3.1E-03	9.6E-04	2.9E-03	1.4E-02	1.4E-02	1.3E-02	9.5E-03	1.2E-02
nbo_L_12	2.8E-02	1.9E-04	4.2E-01	2.1E-04	7.9E-04	**6.3E+00**	4.5E-03	3.2E-03	1.4E-03	2.3E-03
nbo_L_20	4.5E-05	3.9E-05	9.7E-05	3.7E-05	8.1E-05	2.0E-04	1.8E-04	1.6E-04	1.2E-04	1.4E-04
nbo_L_24	9.0E-05	8.1E-05	2.2E-04	8.0E-05	1.9E-04	5.1E-04	4.4E-04	4.1E-04	3.0E-04	3.6E-04
nbo_L_3	4.5E-05	4.0E-05	1.2E-04	5.2E-05	1.0E-04	2.9E-04	2.8E-04	2.8E-04	2.1E-04	2.6E-04
pto_L_12	2.1E-04	1.9E-04	6.2E-04	2.4E-04	6.1E-04	1.7E-03	1.7E-03	1.8E-03	1.4E-03	1.8E-03
pto_L_20	5.9E-05	5.1E-05	1.3E-04	5.0E-05	1.1E-04	2.8E-04	2.4E-04	2.3E-04	1.6E-04	2.0E-04
pto_L_24	8.5E-05	7.1E-05	2.0E-04	6.8E-05	1.6E-04	4.7E-04	3.9E-04	3.7E-04	2.3E-04	3.2E-04
pto_L_3	9.2E-05	8.1E-05	2.5E-04	1.0E-04	2.2E-04	7.0E-04	6.2E-04	6.1E-04	4.4E-04	5.5E-04
rhr_L_12	1.3E-03	2.3E-03	4.8E-03	6.2E-03	1.2E-02	1.8E-02	3.2E-02	4.3E-02	9.2E-02	9.4E-02
rhr_L_24	1.3E-04	1.1E-04	3.8E-04	1.2E-04	3.1E-04	1.2E-03	9.4E-04	8.3E-04	5.5E-04	6.9E-04
rhr_L_3	5.6E-05	2.4E-05	1.5E-04	1.8E-05	5.4E-05	4.0E-04	1.6E-04	1.3E-04	5.3E-05	7.9E-05
sod_L_12	7.5E-05	6.2E-05	1.8E-04	5.9E-05	1.3E-04	4.0E-04	3.2E-04	2.9E-04	1.8E-04	2.4E-04
sod_L_20	5.7E-05	4.8E-05	1.2E-04	4.5E-05	9.2E-05	2.5E-04	2.0E-04	1.8E-04	1.2E-04	1.5E-04
sod_L_3	5.6E-05	4.8E-05	1.3E-04	4.8E-05	1.0E-04	2.9E-04	2.3E-04	2.2E-04	1.4E-04	1.9E-04
ssa_L_15	6.8E-04	4.7E-04	3.7E-03	5.6E-04	2.4E-03	1.9E-02	1.4E-02	1.3E-02	6.3E-03	9.4E-03
ssa_L_21	5.5E-04	4.5E-04	2.9E-03	4.8E-04	2.4E-03	1.2E-02	1.3E-02	1.3E-02	6.6E-03	1.2E-02
ssa_L_4	2.0E-03	1.5E-03	1.6E-02	1.6E-03	1.1E-02	1.1E-01	1.0E-01	9.0E-02	3.4E-02	6.6E-02
ssb_L_15	3.1E-04	1.8E-04	1.2E-03	1.3E-04	5.9E-04	4.4E-03	2.5E-03	1.9E-03	8.0E-04	1.1E-03
ssb_L_21	4.3E-04	3.7E-04	1.8E-03	4.7E-04	1.8E-03	7.9E-03	7.2E-03	7.8E-03	5.0E-03	8.3E-03
ssb_L_4	3.1E-04	2.7E-04	1.2E-03	3.4E-04	1.0E-03	4.5E-03	4.0E-03	3.8E-03	2.5E-03	3.4E-03
tbo_L_12	1.9E-04	1.5E-04	6.5E-04	1.8E-04	5.1E-04	2.3E-03	1.9E-03	1.8E-03	1.0E-03	1.5E-03
tbo_L_20	6.0E-05	5.2E-05	1.3E-04	5.0E-05	1.1E-04	2.9E-04	2.5E-04	2.3E-04	1.6E-04	2.0E-04
tbo_L_24	9.9E-05	8.9E-05	2.4E-04	8.8E-05	2.1E-04	5.8E-04	5.0E-04	4.7E-04	3.4E-04	4.2E-04
tbo_L_3	1.2E-04	1.1E-04	4.2E-04	1.7E-04	3.9E-04	1.4E-03	1.5E-03	1.5E-03	1.1E-03	1.4E-03

Bobbitt, Rosen, Snurr, Fluid Phase Equilibria, 519, 112642, 2020

GCMC results at 300 K, 0.0001 bar
Heat of adsorption in kJ/mol

				DIFF [C5 - X]	
MOF	C5	2-mb	neopent	2-mb	neopent
dia_L_12	-10.1	-8.7	-6.3	-1.5	-3.8
dia_L_20	-8.7	-7.1	-3.0	-1.6	-5.6
dia_L_24	-9.3	-8.3	-5.4	-1.0	-3.9
dia_L_3	-5.9	-6.5	-5.8	0.6	-0.1
lcs_L_12	-11.1	-10.5	-6.9	-0.6	-4.2
lcs_L_3	-7.7	-7.8	-4.2	0.1	-3.6
lvt_L_12	-27.6	-28.5	-24.5	0.9	-3.0
lvt_L_20	-16.6	-16.1	-12.9	-0.5	-3.7
lvt_L_24	-12.8	-13.3	-10.6	0.5	-2.2
lvt_L_3	-23.0	-23.4	-20.6	0.5	-2.4
nbo_L_12	-52.1	-18.1	-13.2	**-34.0**	**-38.9**
nbo_L_20	-9.0	-9.7	-4.6	0.7	-4.3
nbo_L_24	-13.2	-13.2	-9.9	0.0	-3.3
nbo_L_3	-8.9	-9.2	-6.9	0.3	-2.0
pto_L_12	-14.5	-16.3	-12.5	1.7	-2.1
pto_L_20	-9.3	-9.9	-7.1	0.6	-2.1
pto_L_24	-11.0	-10.9	-7.2	0.0	-3.8
pto_L_3	-10.0	-9.9	-7.9	0.0	-2.1
rhr_L_3	-19.4	-11.9	-3.3	-7.5	-16.1
rhr_L_12	-27.2	-31.6	-30.0	**4.4**	**2.7**
rhr_L_24	-16.2	-15.6	-12.0	-0.6	-4.2
sod_L_12	-10.2	-9.7	-5.4	-0.5	-4.8
sod_L_3	-8.9	-7.2	-4.2	-1.7	-4.7
ssa_L_15	-27.0	-25.3	-19.7	-1.6	-7.3
ssa_L_21	-27.7	-28.0	-22.4	0.3	-5.3
ssa_L_4	-35.7	-34.7	-26.8	-1.0	-8.9
ssb_L_15	-24.8	-21.9	-12.2	-2.9	-12.6
ssb_L_21	-23.8	-24.1	-19.6	0.3	-4.2
ssb_L_4	-19.7	-19.6	-16.0	-0.1	-3.7
tbo_L_3	-13.5	-14.4	-12.0	0.8	-1.5
tbo_L_12	-16.2	-15.7	-	-0.5	-
tbo_L_20	-9.6	-9.0	-6.3	-0.6	-3.3

BLUE = favors branched isomer
RED = favors linear isomer

GCMC simulations show that nbo_L12 highly favors linear n-pentane over branched isomers.

Polymorph family:

lvt/nbo/rhr

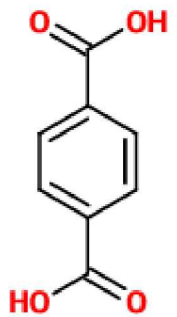

L12

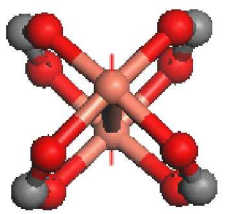

Cu paddlewheel node

rhr_L12 polymorph shows slight selectivity for the branched isomers

We will focus on these three polymorphs.

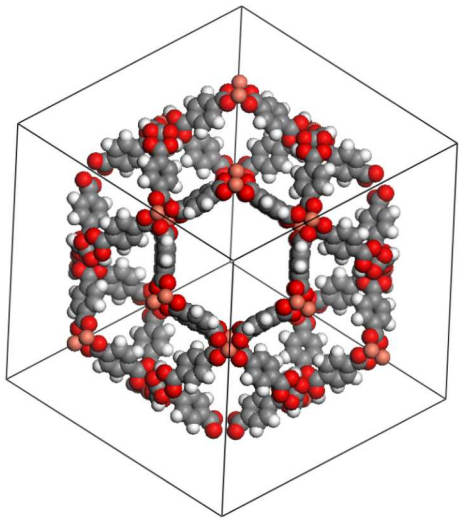

rhr_L12

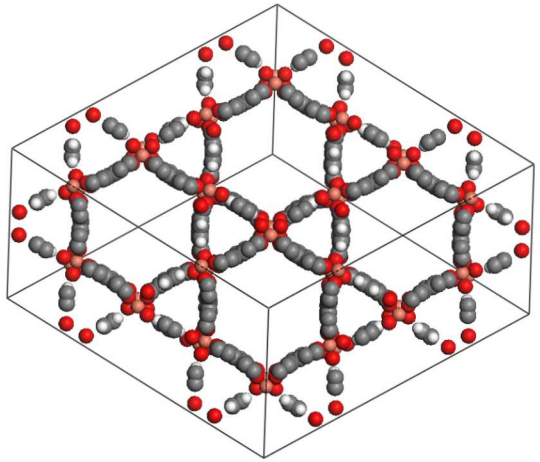

nbo_L12

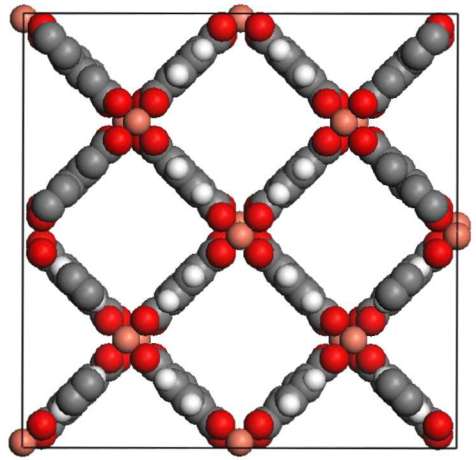

lvt_L12

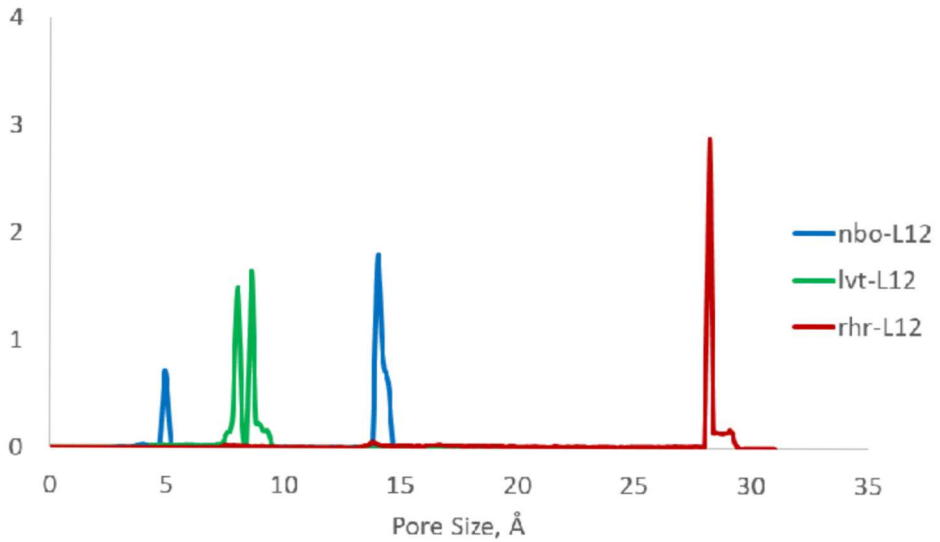

MOF	Pore size (Å)
rhr_L12	28.2
nbo_L12	4.9, 14.0
lvt_L12	8.0, 8.6

The small pores in nbo_L12 will accommodate n-hexane but exclude bulkier branched isomers.

Alkane	X	Y	Z	Kinetic Dia. (Å)
n-hexane	9.7	4.5	4.0	4.3
2-methylpentane	9.2	6.2	5.2	5.0
3-methylpentane	9.3	6.2	5.2	5.0
2,2-dimethylbutane	8.0	6.7	5.9	6.2
2,3-dimethylbutane	7.8	6.7	5.3	5.6

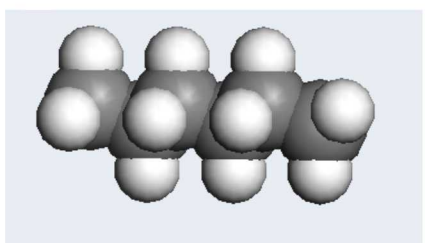

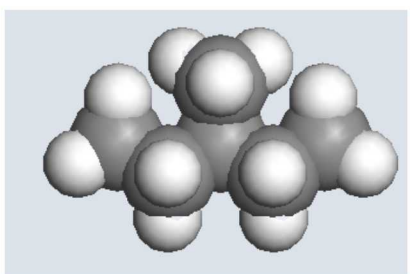

nbo_L12

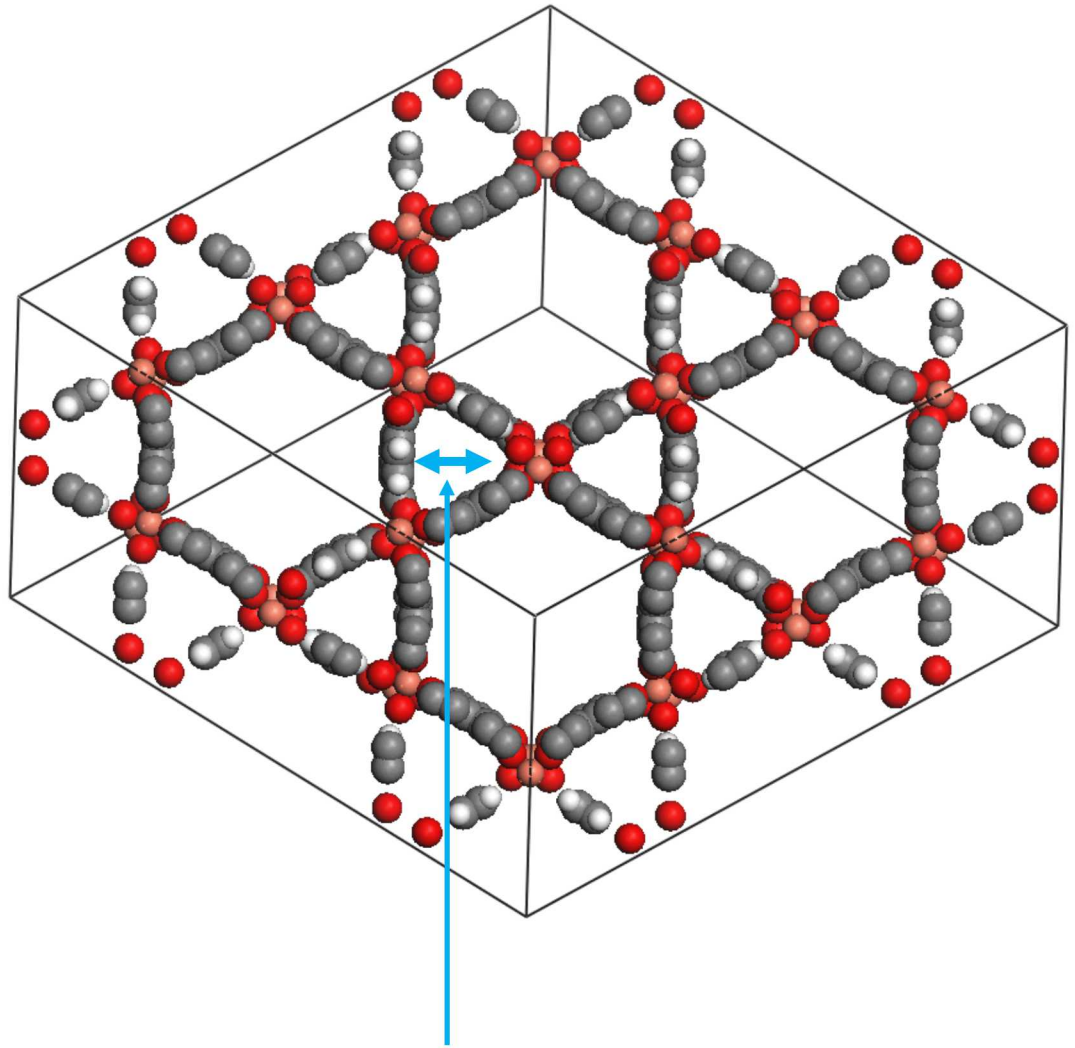

Alkane diameters: Peralta, Ind. Eng. Chem. Res., 2012,51, 4692-4702

n-hexane
300 K

Linear molecules prefer the small pores at low pressure.

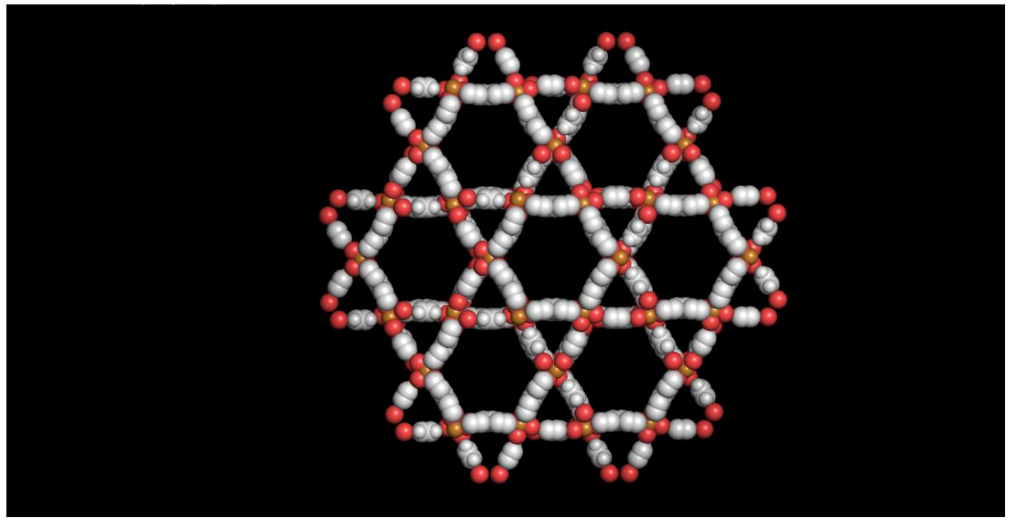

No adsorbate

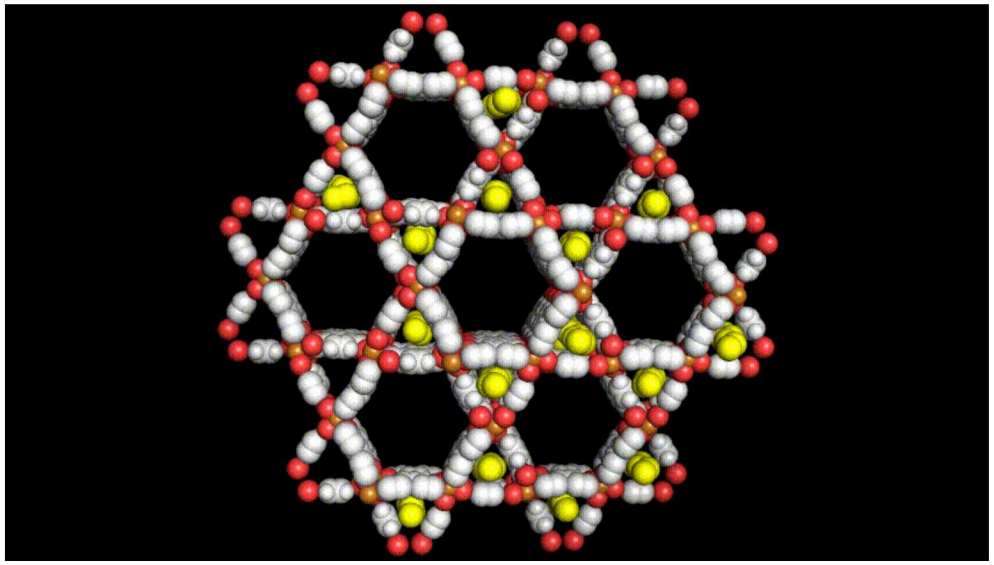

10 Pa

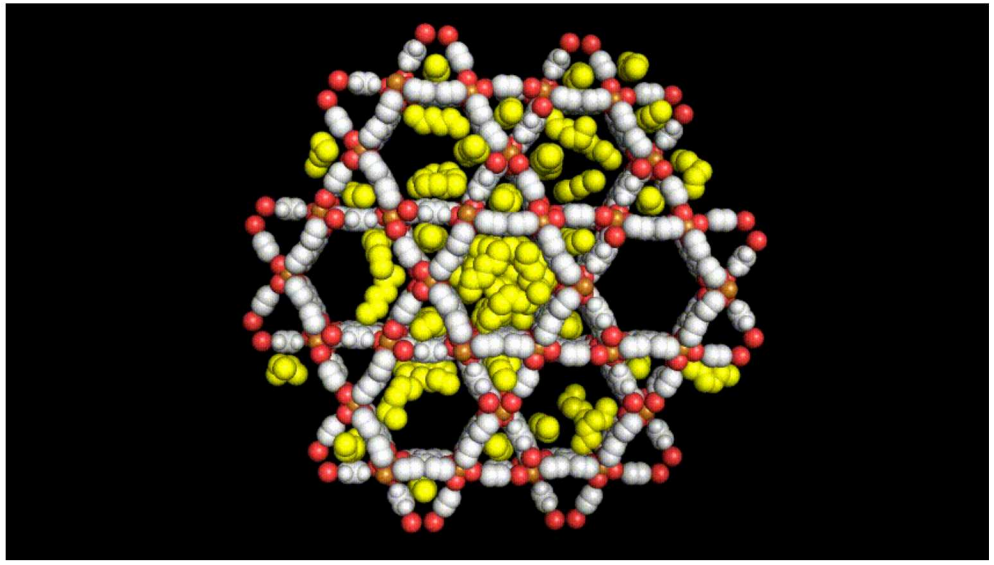

100 Pa

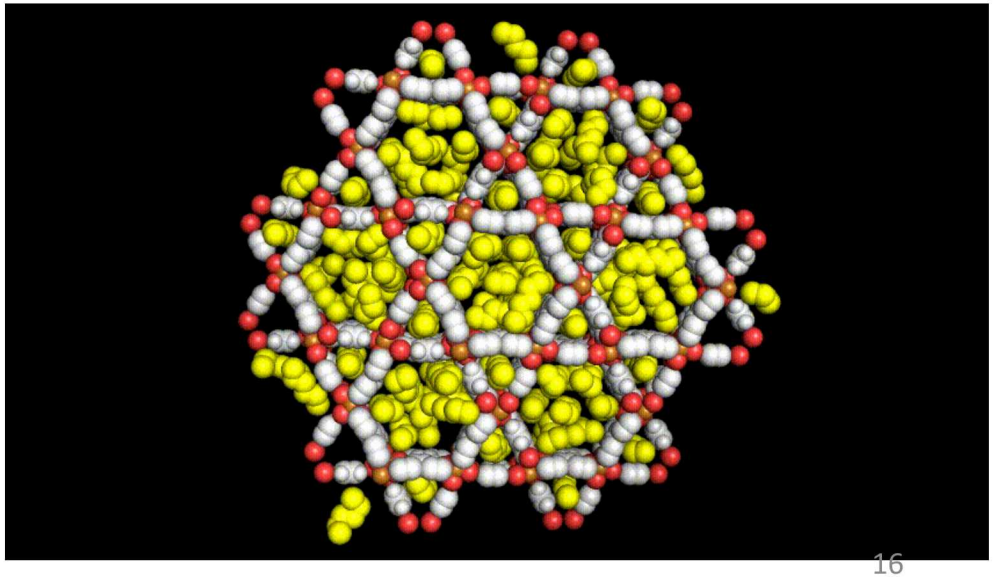

1000 Pa

Bobbitt, Rosen, Snurr, Fluid Phase Equilibria, 519, 112642, 2020

At low pressure, the monobranched isomer prefers the large pores

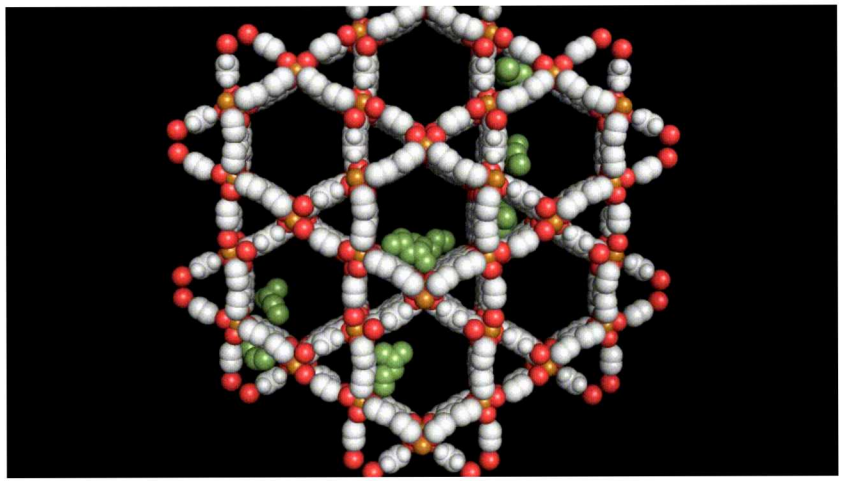

100 Pa

At saturation, 2-mp can be forced into the small triangle pore

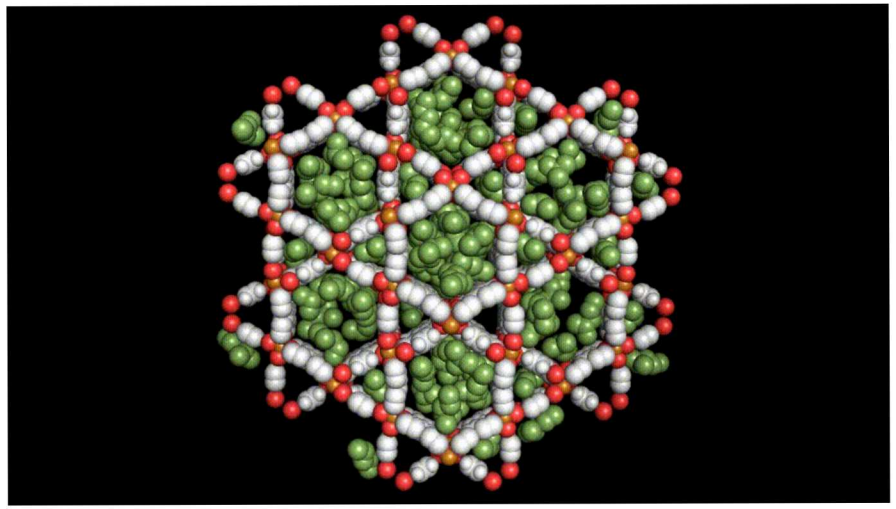

1000 Pa

2-methylpentane
300 K

Bobbitt, Rosen, Snurr, Fluid Phase Equilibria, 519, 112642, 2020

23-dmb cannot go into the small pore even at high pressure

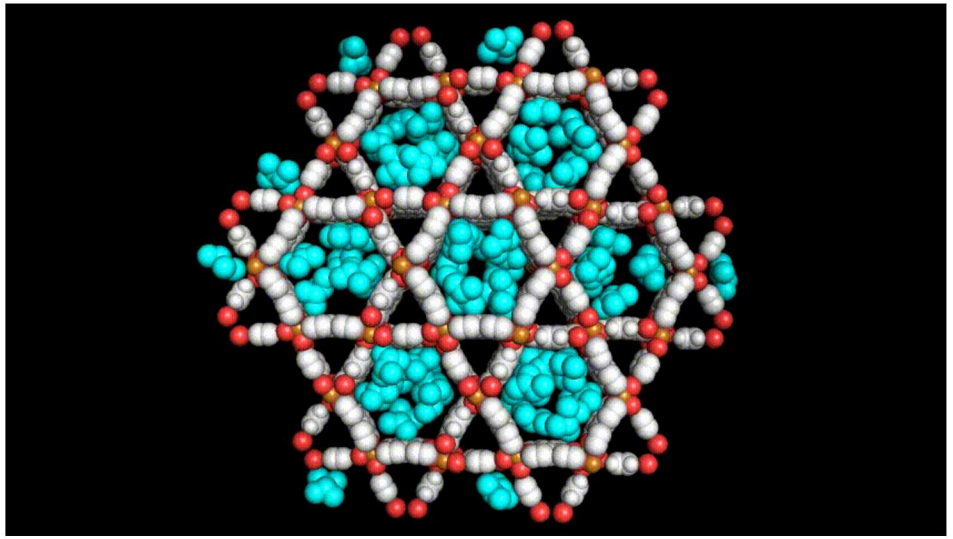

1000 Pa

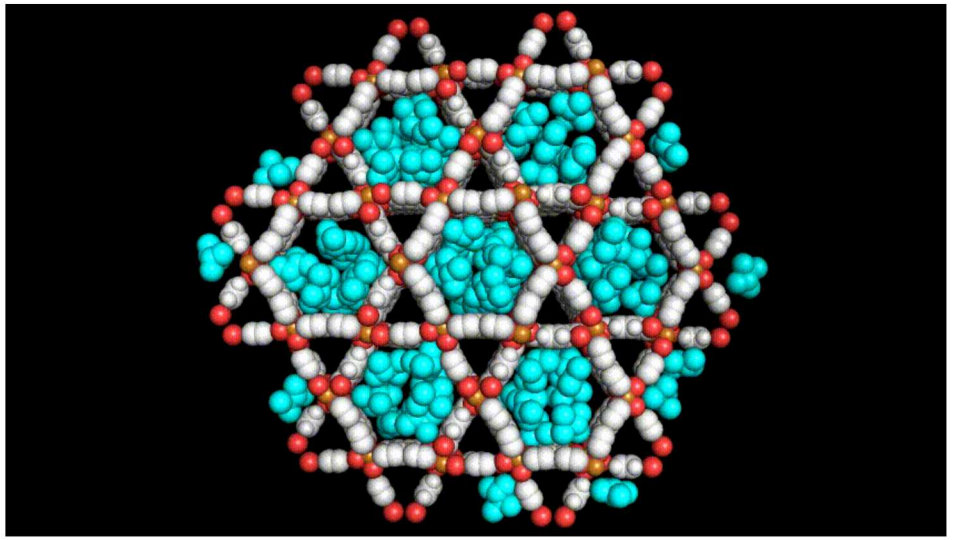

10000 Pa

2,3-dimethylbutane
300 K

Bobbitt, Rosen, Snurr, Fluid Phase Equilibria, 519, 112642, 2020

2,3-dimethylbutane

n-hexane

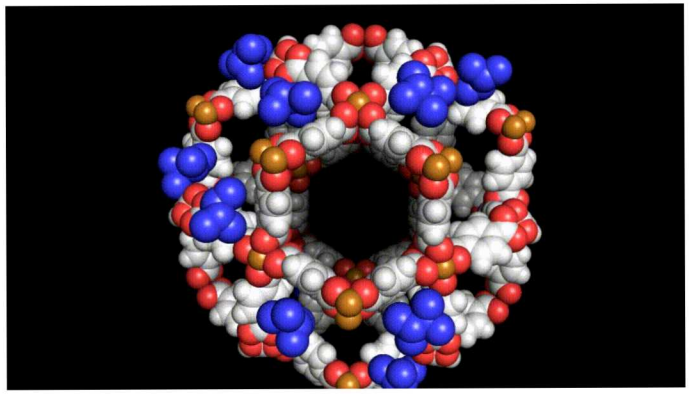

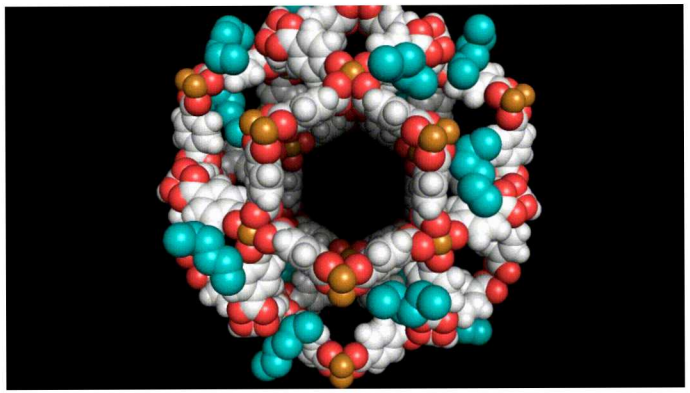

100 Pa

In rhr_L12, the molecules first go to the windows surrounding the large spherical pore

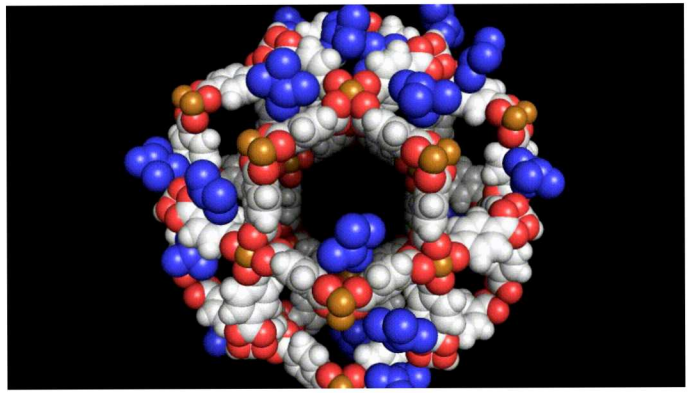

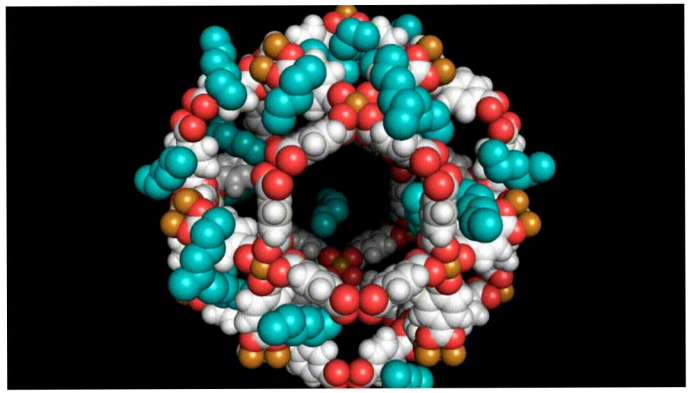

1000 Pa

At higher pressure, the pore is filled.

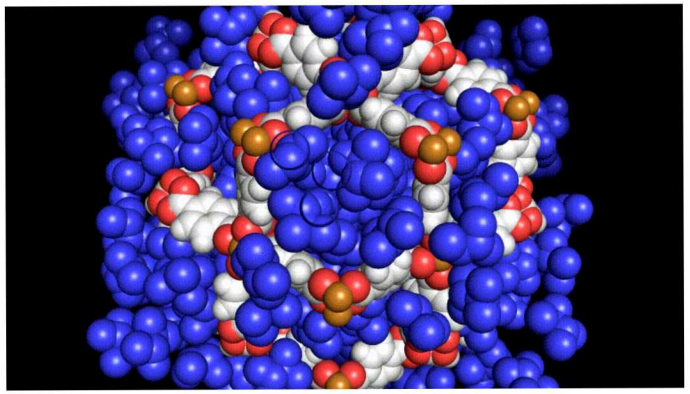

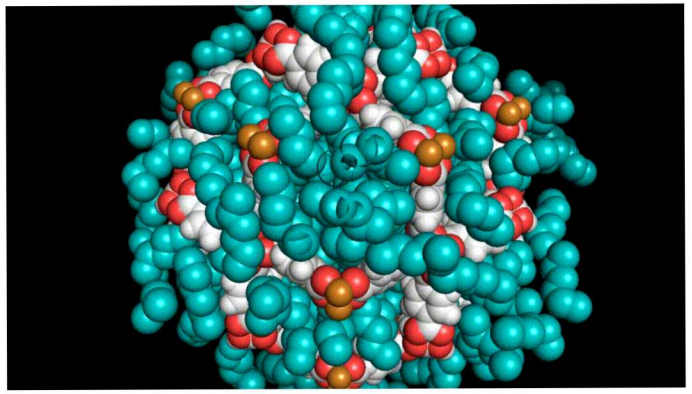

10,000 Pa

MOF nbo-L12 shows selectivity for n-pentane at low pressure. 2-methylbutane is adsorbed into the small pores.

At saturation, there is less neopentane because it is excluded from the small pores.

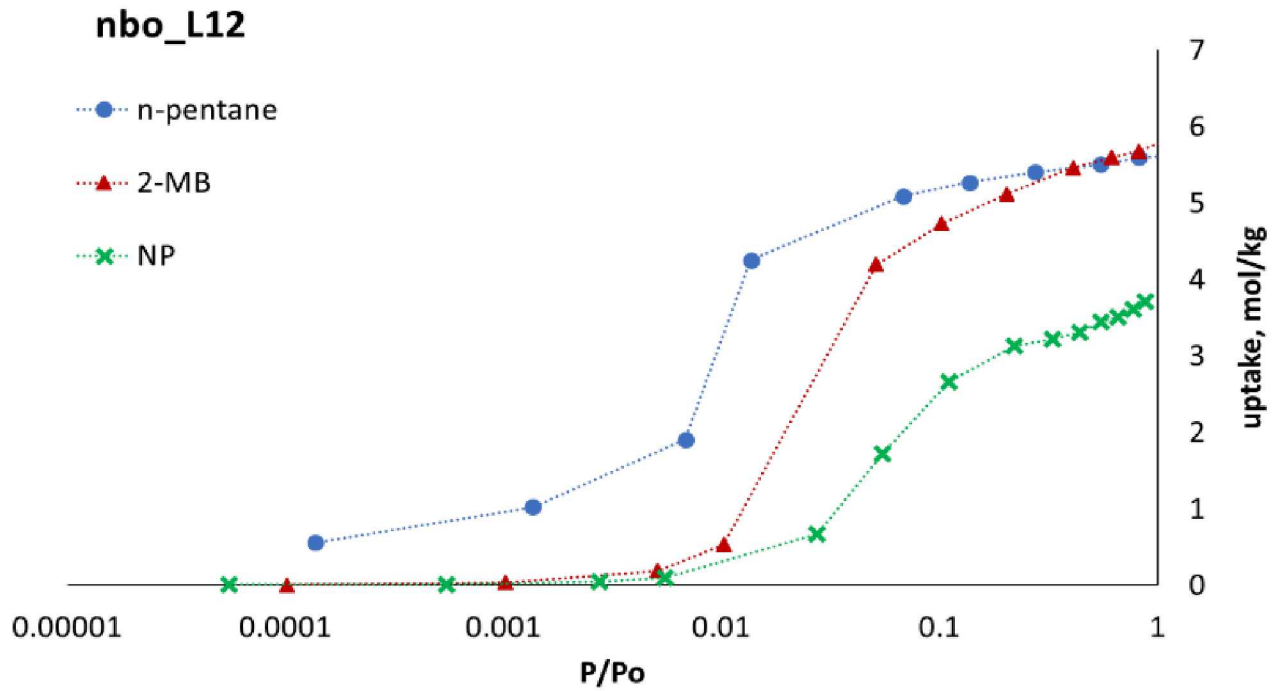

0.1 bar

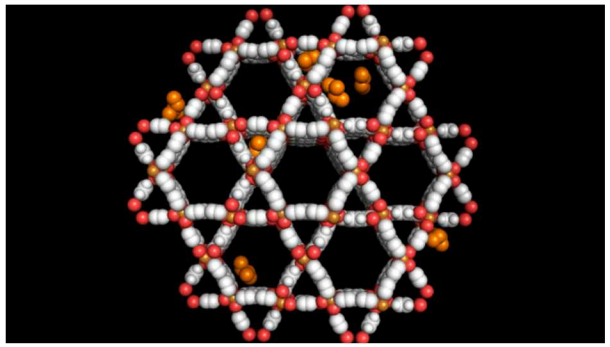

1.0 bar

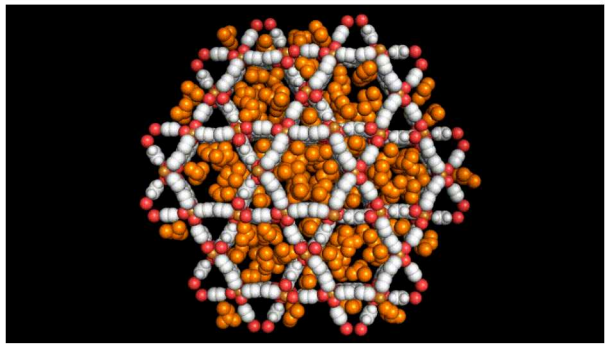

2-methylbutane
300 K
Single component isotherms

Bobbitt, Rosen, Snurr, Fluid Phase Equilibria, 519, 112642, 2020

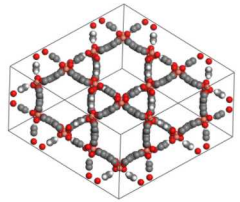

nbo

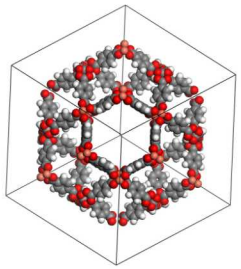

rhr

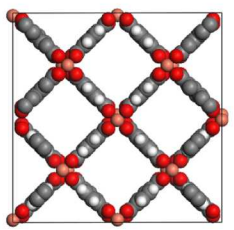

lvt

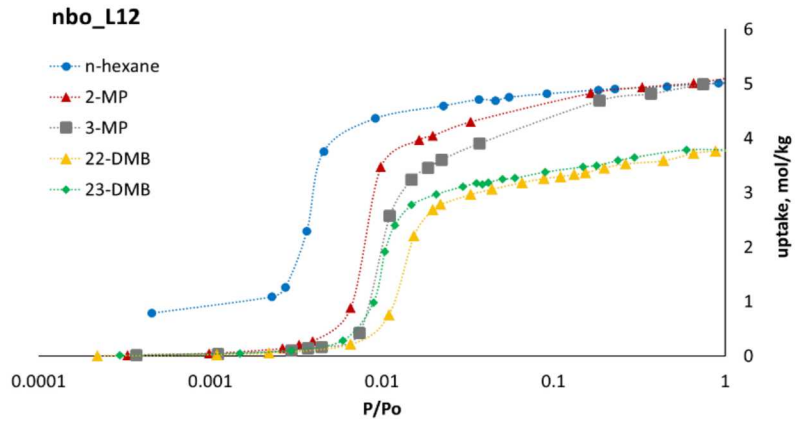

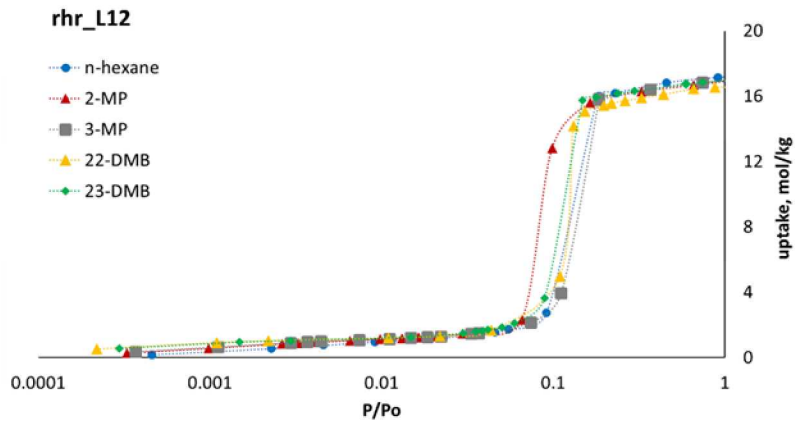

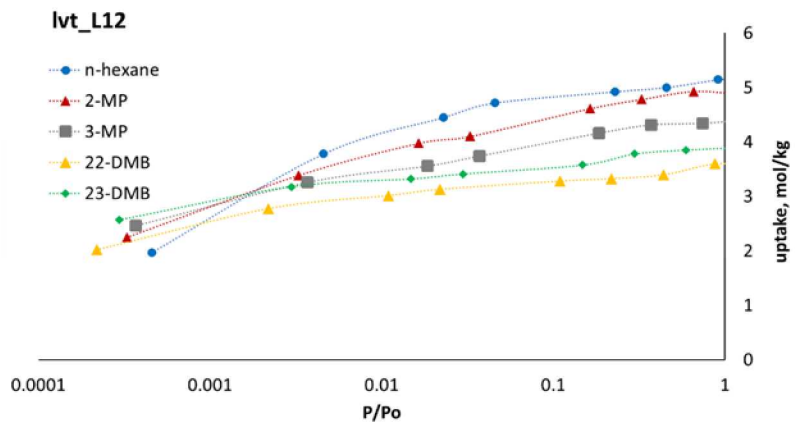

In nbo MOF, we see a separation of linear and 1-methyl isomers from dimethyl isomers.

No separation in the large pore rhr MOF.

lvt MOF shows reduction in bulkier molecules due to packing in the square pores

C6 isomers
300 K

Bobbitt, Rosen, Snurr, Fluid Phase Equilibria, 519, 112642, 2020

Multi-component Adsorption

GCMC simulations for a 5-component mixture containing all C6 isomers.
433 K, 1 bar 100k/100k cycles

Adsorbate	Selectivity
n-hexane	2.8
2-MP	0.79
3-MP	0.76
23-DMB	0.74
22-DMB	0.51
(L+MP)/DMB	1.86

Equimolar mixture

Linear + monobranched selectivity: 1.86

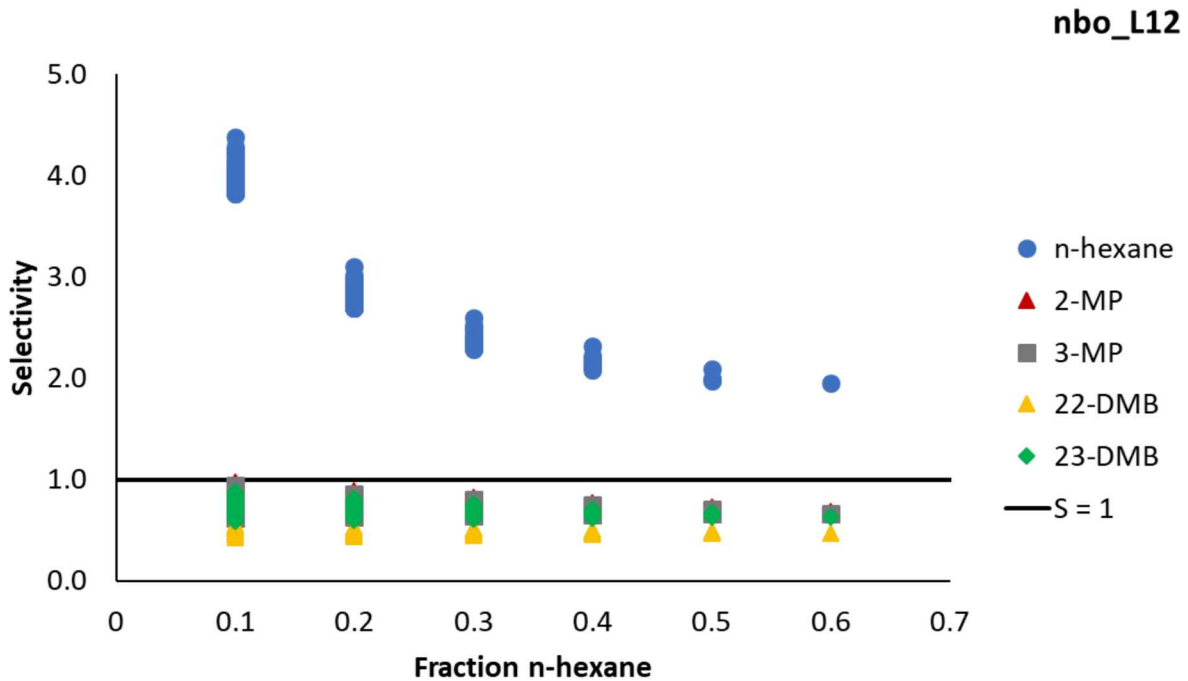

nC6 selectivity goes down when it forms a higher fraction of mixture

Bobbitt, Rosen, Snurr, Fluid Phase Equilibria, 519, 112642, 2020

Thermodynamics

	H_ads				ΔH_ads [linear-X]		
	300 K	kJ/mol			300 K	kJ/mol	
	nbo_L12	rhr_L12	lvt_L12		nbo_L12	rhr_L12	lvt_L12
C5	-65.3	-36.9	-36.1		0.0	0.0	0.0
2-methylbutane	-30.1	-40.7	-36.7		35.2	-3.8	-0.6
neopentane	-23.7	-38.7	-33.0		41.6	-1.8	3.1
C6	-76.7	-41.6	-42.5		0.0	0.0	0.0
2-methylpentane	-40.4	-44.6	-42.6		36.4	-2.9	-0.1
3-methylpentane	-36.7	-45.7	-42.9		40.0	-4.1	-0.4
22-dimethylbutane	-29.9	-47.8	-42.1		46.8	-6.1	0.5
23-dimethylbutane	-31.8	-48.3	-43.5		44.9	-6.7	-1.0

RED: more favored than linear alkane
BLUE: less favored than linear alkane

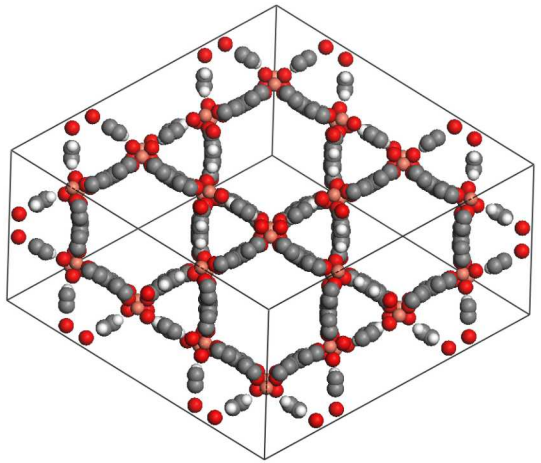

Changing the topology can flip the trends in selectivity

Enthalpy of adsorption shows that nbo MOF is more selective for n-hexane by ~40 kJ/mol

rhr MOF shows some slight selectivity for the branched isomers over the linear isomer

There is very little selectivity for the lvt MOF

Thermodynamics

Calculated from Henry constant data.

	TdelS				A_ads		
	kJ/mol, 300 K				kJ/mol, 300 K		
	nbo_L12	rhr_L12	lvt_L12		nbo_L12	rhr_L12	lvt_L12
C5	33.8	18.4	11.6		-34.0	-21.0	-27.0
2-methylbutane	11.0	19.6	11.0		-15.2	-21.6	-24.5
neopentane	14.8	20.7	11.6		-17.8	-22.5	-27.6
Spread [max - min]	22.7	2.3	0.7		18.8	1.5	3.0
C6	38.2	19.8	13.3		-41.1	-24.3	-31.7
2-methylpentane	20.1	21.5	13.0		-22.7	-25.5	-32.1
3-methylpentane	17.1	21.7	12.7		-22.1	-26.5	-32.7
22-dimethylbutane	12.4	22.0	12.4		-20.0	-28.3	-32.2
23-dimethylbutane	13.2	22.4	12.7		-21.1	-28.4	-33.3
Spread [max - min]	25.7	2.6	1.0		21.1	4.1	1.6

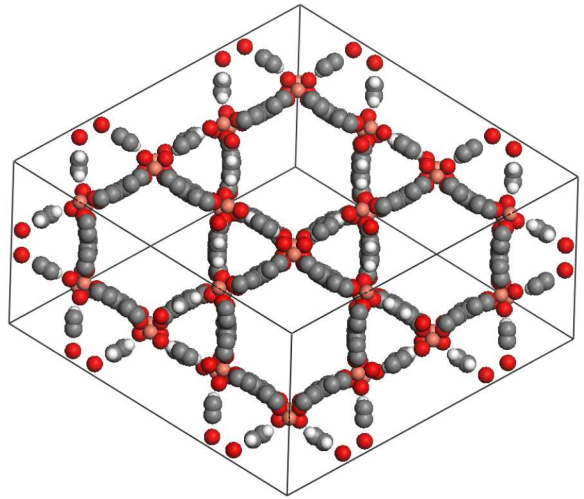

Large entropy penalty for adsorption of linear isotherms in nbo_L12

The rhr and lvt MOFs show little differentiation based on entropy.

The slight selectivity for branched isomers in the rhr MOF is driven by enthalpy.

The nbo topology has two distinct conformations that are the same topology.

nbo cube

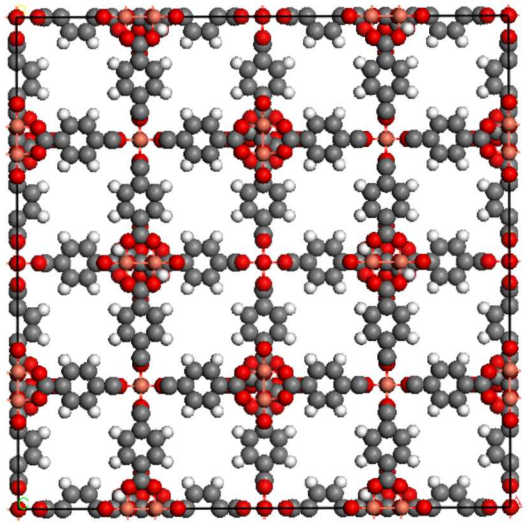

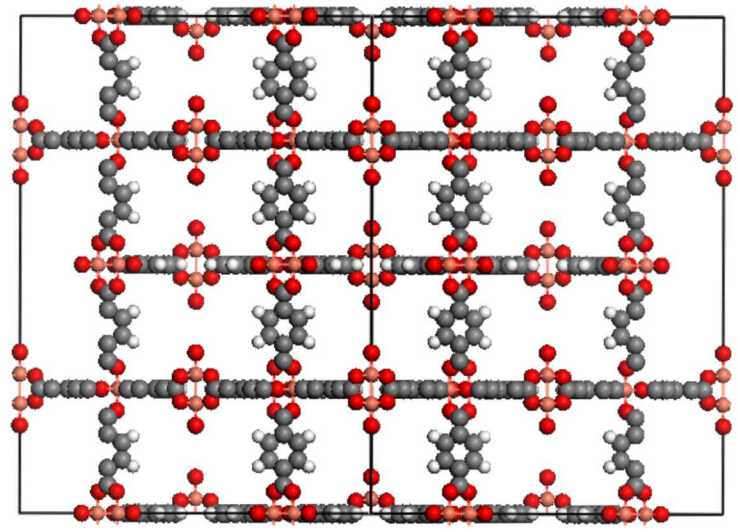

nbo star

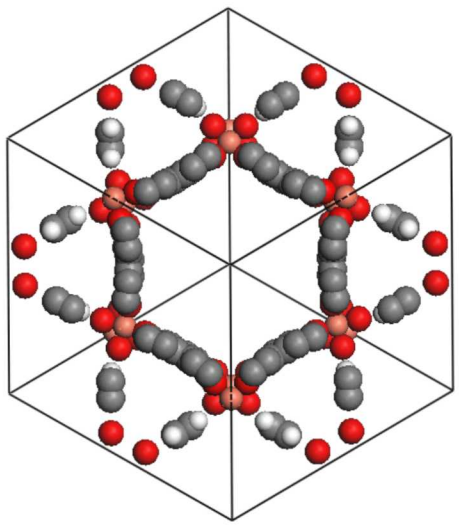

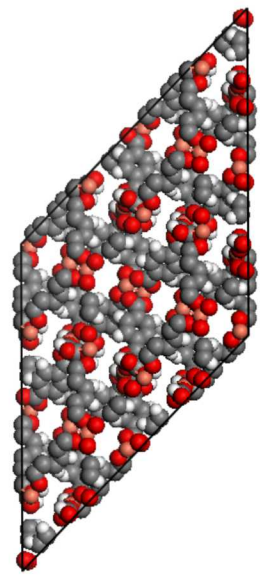

simplified nbo topology

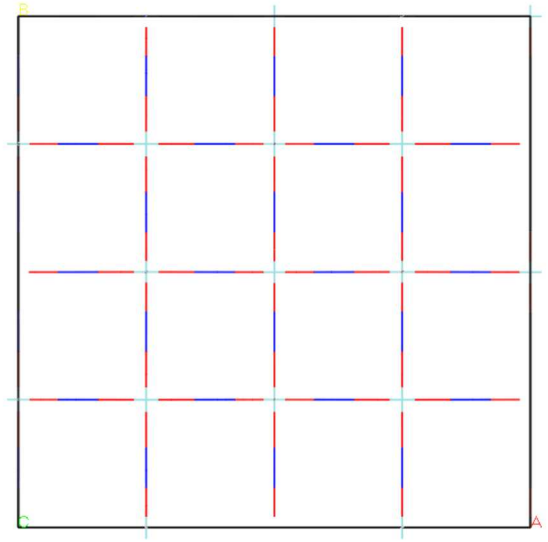

The connectivity is the same in each conformation. The simplified maps are equivalent.

nbo cube

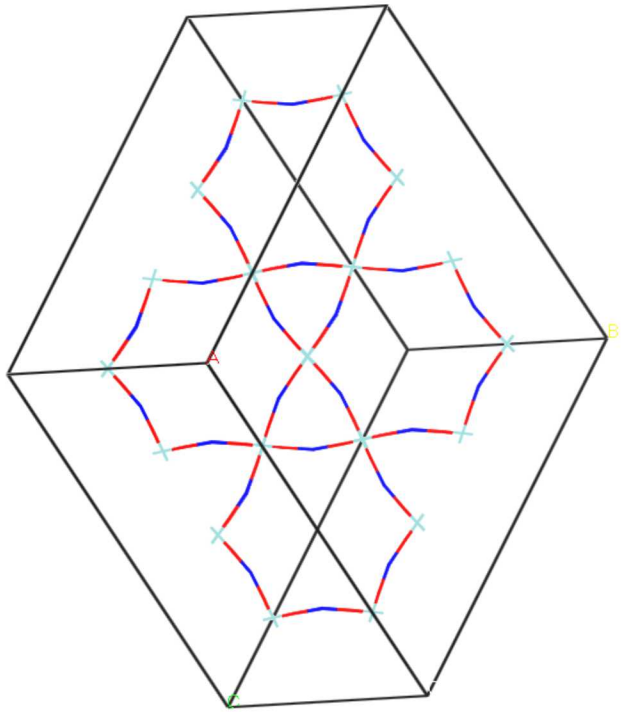

nbo star

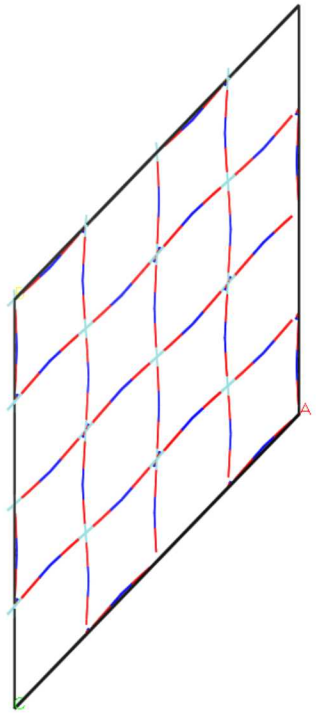

You can see how the star confirmation forms by looking down the [111] view of the cube confirmation.

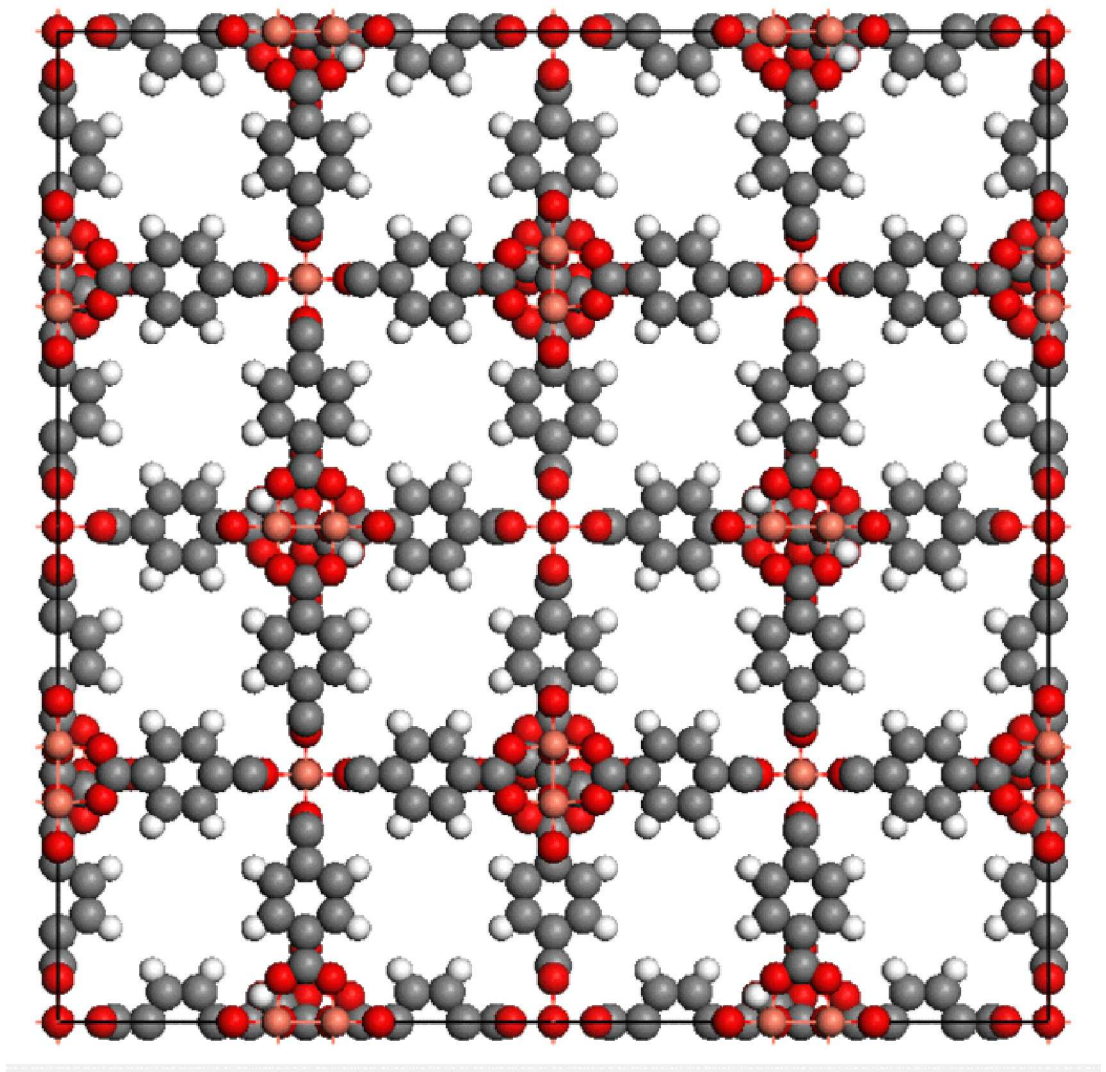

The star confirmation seen in MOF nbo_L12 is formed by compressing the MOF along the [111] axis so the

Cu-Cu vectors in alternating directions

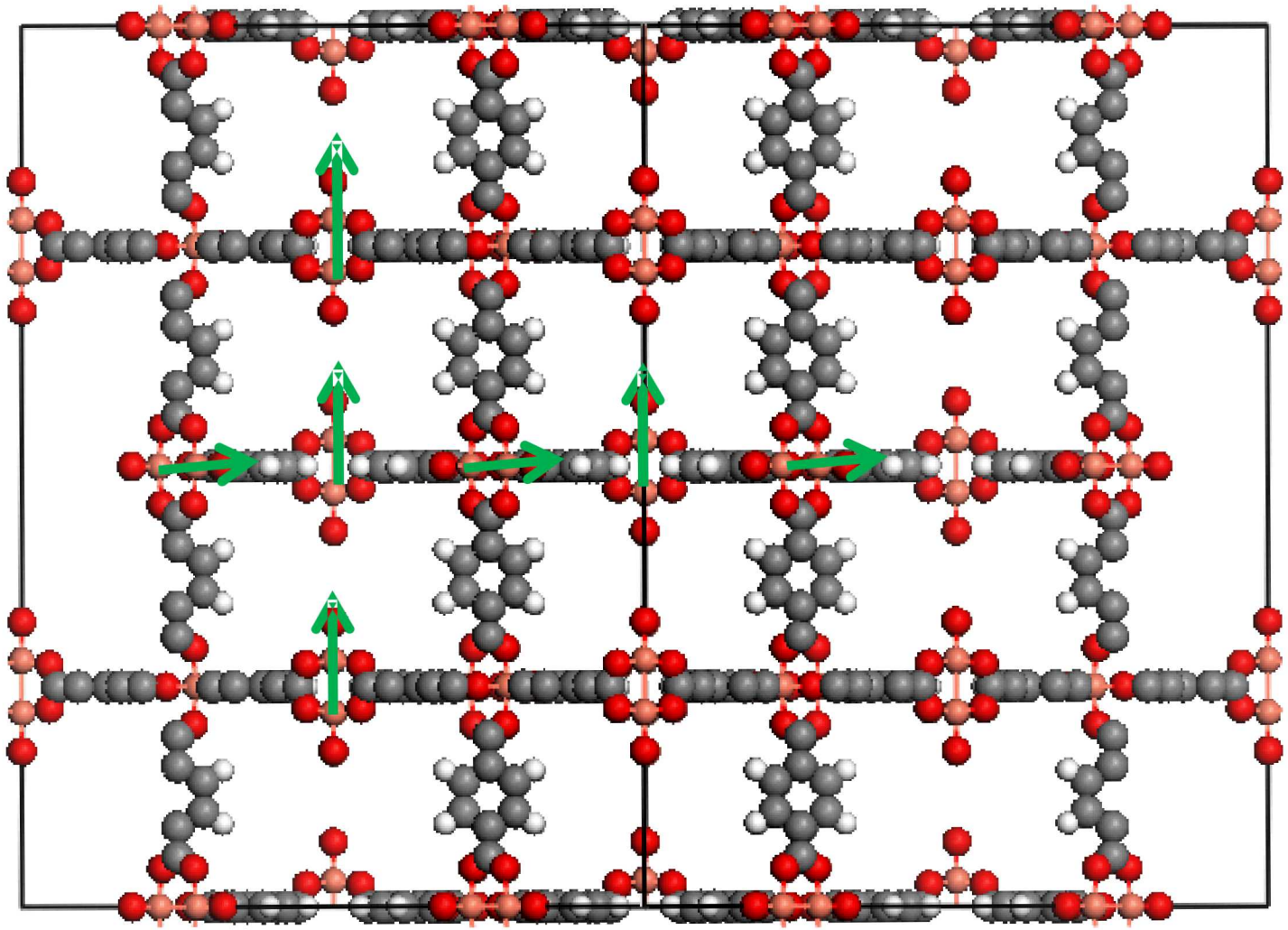

In square nbo confirmation the Cu paddlewheel nodes are aligned normal to their nearest neighbor node.

Cu-Cu torsion angle ~35 degrees

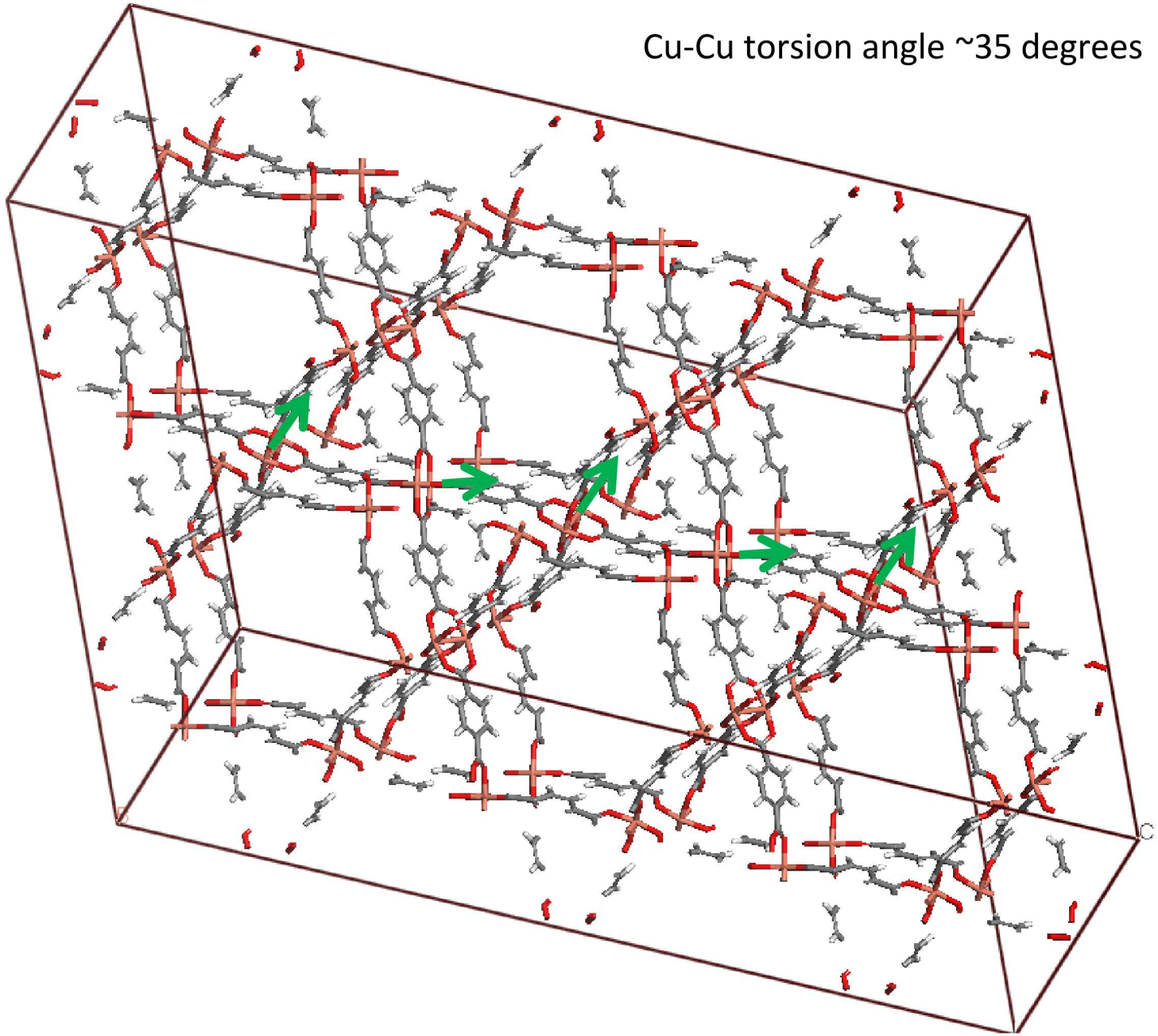

In the nbo star confirmation the Cu paddlewheel nodes are twisted to a 35 degree angle from their neighbors.

Geometrical minimization of MOF nbo_L12

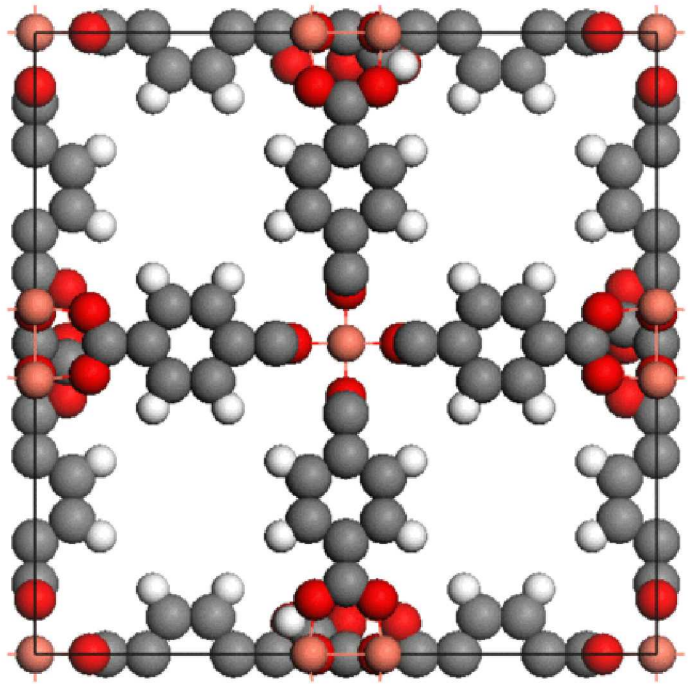

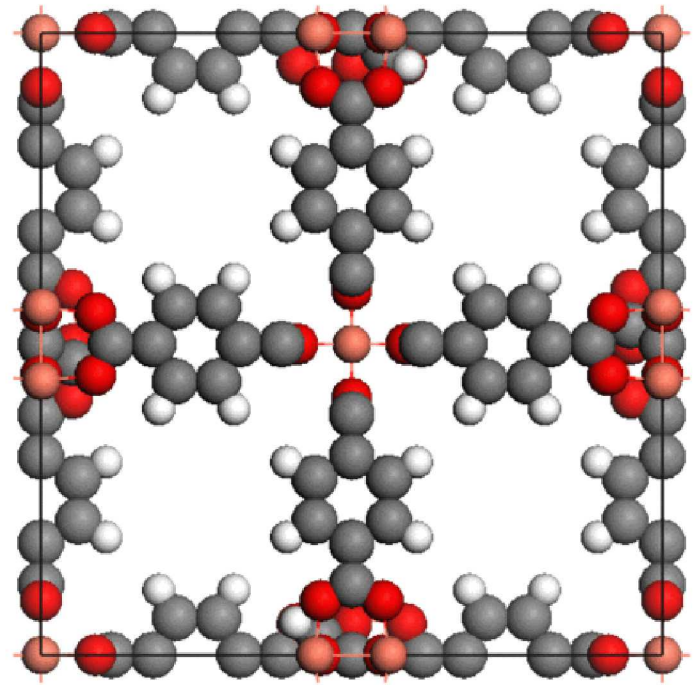

The conformation is determined by steric hindrance between the linker and node.

L12

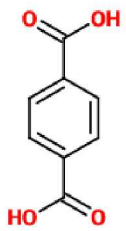

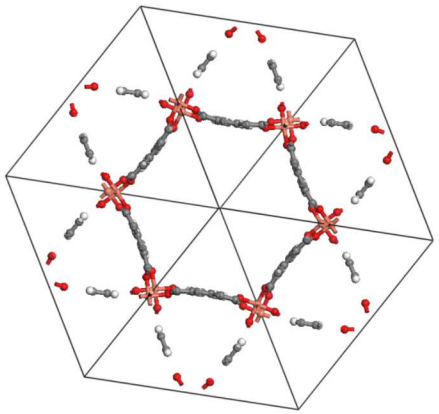

L20

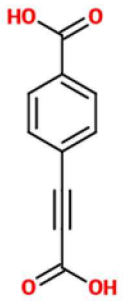

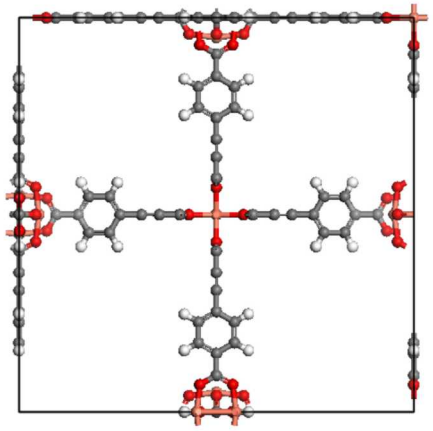

When the nodes are weakly coupled by hindrance the MOF takes on a slightly skewed confirmation.

L24

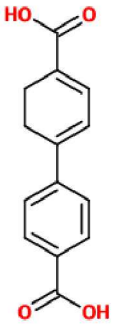

L22

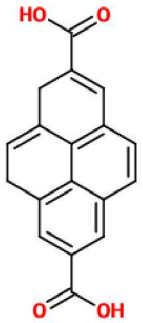

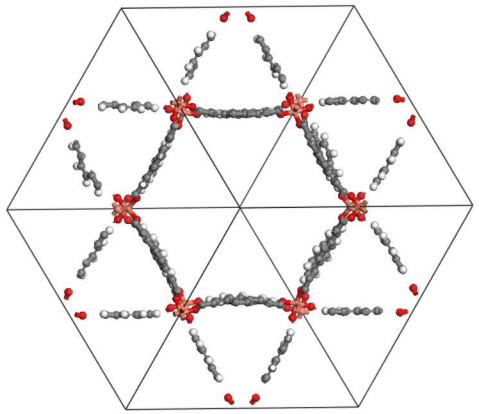

L34

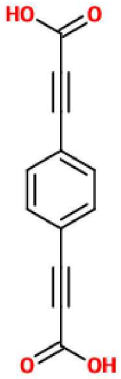

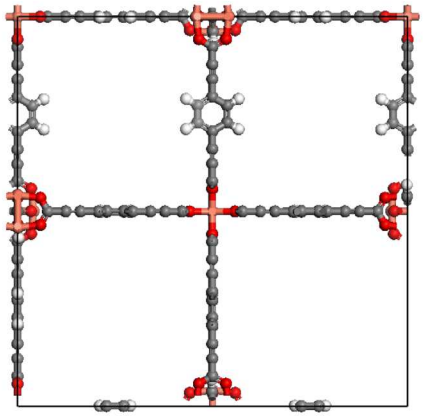

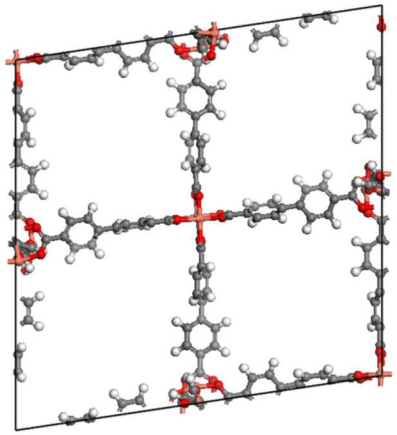

Bobbitt, Rosen, Snurr, Fluid Phase Equilibria, 519, 112642, 2020

DFT calculations show that the star confirmation is more favorable for certain linkers.

VASP v5.4
PBE-D3(BJ) with PAW pseudopotentials from VASP
520 eV cutoff
Spin polarized with antiferromagnetic alignment of Cu atoms

L12

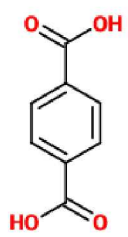

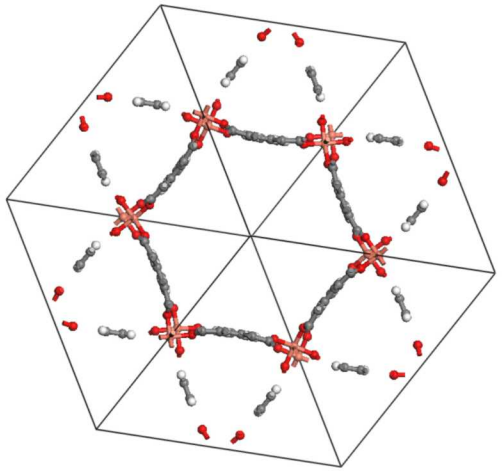

32 kJ/mol (per formula unit) more favorable than square

L22

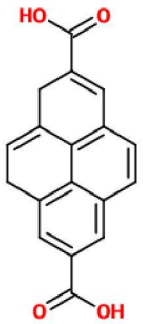

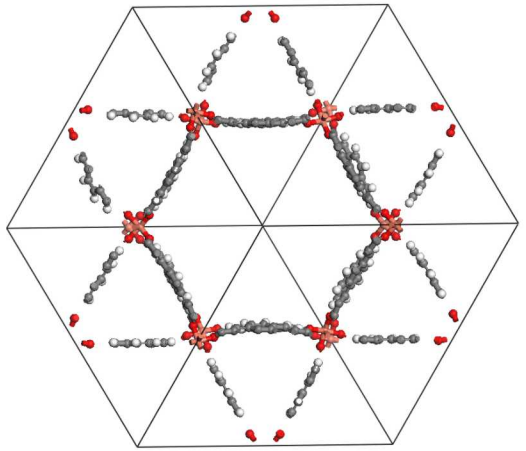

14 kJ/mol (per formula unit) more favorable than square

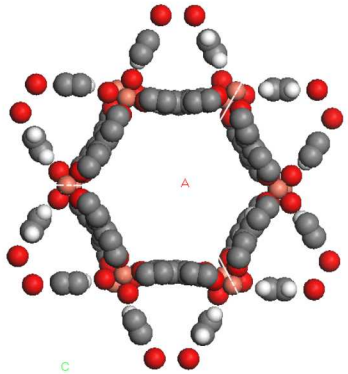

nbo

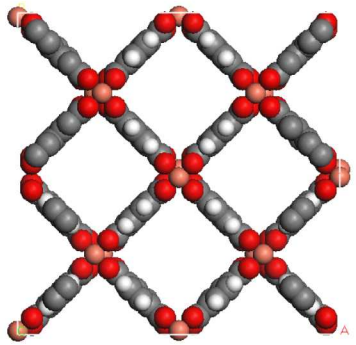

lvt

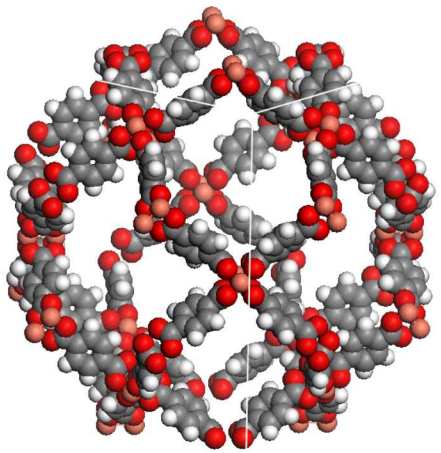

rhr

MOF	UFF	DFT
nbo_L12	0	0
lvt_L12	-1.2	12.2
rhr_l12	17.7	-

kJ/mol per formula unit

According to UFF optimizations, lvt_L12 is most favorable closely followed by nbo_L12, with rhr_L12 significantly less favorable.

Based on DFT, nbo_L12 is more favorable than lvt_L12.
(rhr_L12 unit cell was too large for DFT)

*based on UFF optimization in Materials Studio and DFT optimization in VASP

Bobbitt, Rosen, Snurr, Fluid Phase Equilibria, 519, 112642, 2020

Conclusions

1. Topology can greatly affect MOF pore size and shape, which has implications for separations

2. nbo/lvt/rhr polymorph family has different linear/branched selectivity depending on topology

3. nbo MOFs with phenyl ring linker show high selectivity for linear alkanes due to small pores

4. nbo topology can form different conformations (cube vs star) depending on steric effects of the linker

Acknowledgements:

This work was supported by the US Department of Energy under Award DE-FG02-08ER15967.

U.S. DEPARTMENT OF ENERGY

SAND2019-13769 C

Bobbitt, Rosen, Snurr, Fluid Phase Equilibria, 519, 112642, 2020